AD-A061 630 NAVAL RESEARCH LAB WASHINGTON D C F/G 20/9
A FINITE-CIRCUIT-ELEMENT CODE FOR MODELING THE DYNAMICS OF A GY--ETC(U)
MAY 78 D L BOOK, P J TURCHI, D L STEIN

UNCLASSIFIED NRL-MR-3827 NL

1 OF 1
AD A061630

END
DATE FILMED
2 - 79
DDC

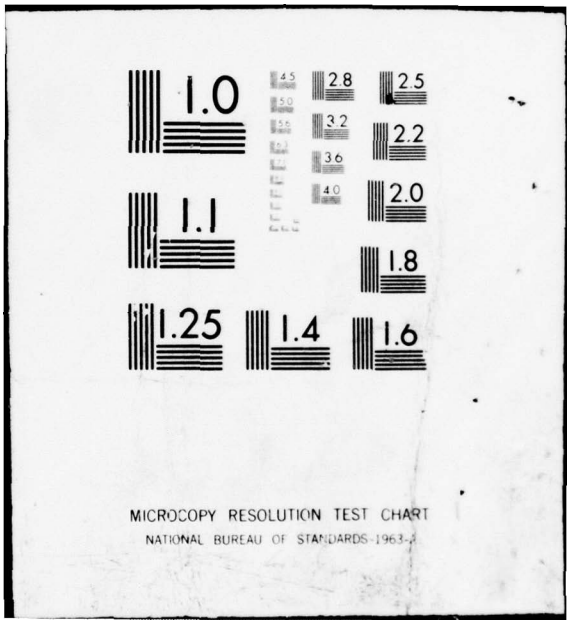
1.0
1.1
1.25
1.4
1.6
1.8
2.0
2.2
2.5
2.8
3.2
3.6
4.0
4.5
5.0
MICROCOPY RESOLUTION TEST CHART
NATIONAL BUREAU OF STANDARDS-1963-A

NRL Memorandum Report 3827

A Finite-Circuit-Element Code for Modeling the Dynamics of a Gyrating Charged-Particle Beam

D.L. Book

Laboratory for Computational Physics

P.J. Turchi

Plasma Physics Division

and

D.L. Stein

Joseph Henry Laboratory, Princeton University
Princeton, NJ 08540

May, 1978

This work was sponsored by the Office of Naval Research under Project RR011-09.

NAVAL RESEARCH LABORATORY
Washington, D.C.

SECURITY CLASSIFICATION OF THIS PAGE (When Data Entered)

REPORT DOCUMENTATION PAGE

READ INSTRUCTIONS BEFORE COMPLETING FORM

1. REPORT NUMBER (14) NRL-MR- 2. GOVT ACCESSION NO. 3. RECIPIENT'S CATALOG NUMBER (9)

NRL Memorandum Report 3827

4. TITLE (and Subtitle) (6)

A FINITE-CIRCUIT-ELEMENT CODE FOR MODELING THE DYNAMICS OF A GYRATING CHARGED-PARTICLE BEAM *

5. TYPE OF REPORT & PERIOD COVERED

Interim report on a continuing NRL Problem.

6. PERFORMING ORG. REPORT NUMBER

7. AUTHOR(s) (10)

David L. Book, P. J. Turchi, and D. L. Stein

8. CONTRACT OR GRANT NUMBER(s)

9. PERFORMING ORGANIZATION NAME AND ADDRESS

Naval Research Laboratory
Washington, D. C. 20375

10. PROGRAM ELEMENT, PROJECT, TASK AREA & WORK UNIT NUMBERS

NRL Problem No. 77HO2-51
ONR Project No. RR011-09

11. CONTROLLING OFFICE NAME AND ADDRESS (11)

Office of Naval Research
800 N. Quincy Street
Arlington, Virginia 22217

12. REPORT DATE (12)

May 1978

13. NUMBER OF PAGES

45

14. MONITORING AGENCY NAME & ADDRESS (if different from Controlling Office)

(12) 68 p.

15. SECURITY CLASS. (of this report)

UNCLASSIFIED

15a. DECLASSIFICATION/DOWNGRADING SCHEDULE

16. DISTRIBUTION STATEMENT (of this Report)

Approved for public release; distribution unlimited.

17. DISTRIBUTION STATEMENT (of the abstract entered in Block 20, if different from Report)

18. SUPPLEMENTARY NOTES

* Joseph Henry Laboratory, Princeton University, Princeton, NJ 08540

This project was sponsored by Office of Naval Research, Project No. RR011-09.

19. KEY WORDS (Continue on reverse side if necessary and identify by block number)

Liners
Charged-Particle Rings
Field-Reversal
Finite Element Simulation

20. ABSTRACT (Continue on reverse side if necessary and identify by block number)

A method is described for calculating the interaction between an imploding liner, a magnetically confined charged particle ring (Astron e-layer, ion ring) and a target plasma, based on the equations of the equivalent circuit. Expressing the electrodynamical behavior in terms of inductive coupling between circular current loops, so that changes in geometry and plasma parameters are described by changes in the induction coefficients, means that only ordinary differential equations arise, in contrast with fluid descriptions. Induced electron currents are conveniently included in the model. Application to a beam-target fusion system driven by the compression of an ion ring is described as a illustration of the utility of the technique.

DD FORM 1 JAN 73 1473 EDITION OF 1 NOV 65 IS OBSOLETE
S/N 0102-014-6601

SECURITY CLASSIFICATION OF THIS PAGE (When Data Entered)

251950

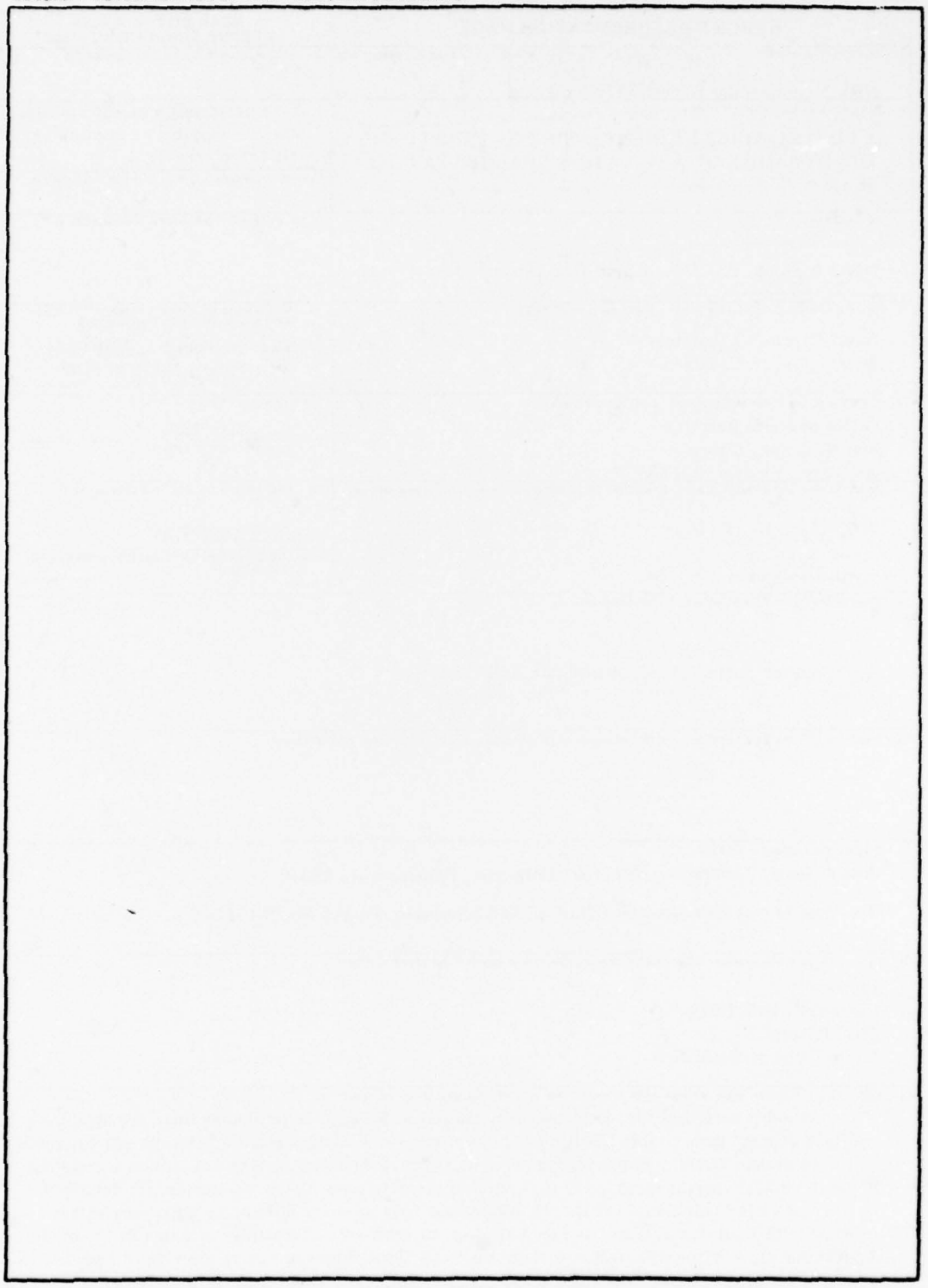

CONTENTS

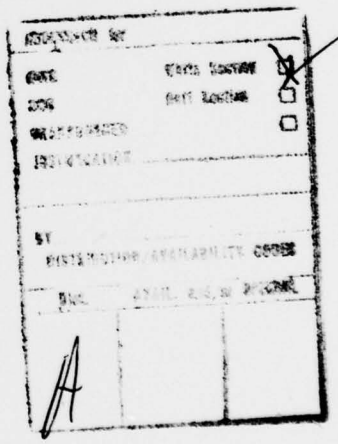

A FINITE-CIRCUIT-ELEMENT CODE FOR MODELING THE COMPRESSION OF A GYRATING CHARGED-PARTICLE BEAM

I. INTRODUCTION

Over the last several years a great deal of interest has arisen in connection with the topic of gyrating intense ion beams.[1-3] A ring or cylindrical current layer is produced by the motion of the ions in the superposed background (quasiuniform) magnetic field and the poloidal self-field, with ring major radius R equal to the ion gyroradius. If the net current in such a configuration is strong enough, the direction of the field lines within the ring can be opposite that of the background field (Fig. 1). When the poloidal field on axis, $B_p = \mu_o I / 2R$, exceeds the background field B_o, the field in the interior region is completely reversed.

Recently it has been proposed to increase the intensity of the neutral beams used to heat the plasma in 2xIIB and similar mirror devices in order to produce field reversal.[4] As pointed out by Baldwin and Rensink,[5] electric fields induced by the buildup of current tend to partially cancel the ion current. It is thus unclear that an initially unreversed configuration can become reversed, no matter how much ion current is added. Even if the configuration is compressed radially (by the action, e.g., of external coils, an imploding liner, or axial translation in a tank with converging metal walls), field reversal is problematic. The flux linking the ion ring tends to be conserved, and collisional diffusion only flattens the profiles.

Manuscript submitted July 19, 1978.

The present paper describes a code developed for treating the dynamics of a gyrating ion ring interacting with a background plasma and a (possibly imploding) metal liner. The code is called IPICAC (for Ion Beam-Plasma Interaction with Cylindrical Adiabatic Compression). It is two-dimensional (in r, z) and assumes axisymmetry, but does not employ finite-differences on a 2D grid to solve the dynamical problem. Instead, each portion of the system which carries current is regarded as part of a circular current loop. The beam is one such loop; the liner or wall may be approximated by several loops side by side. These current loops are coupled by their mutual inductances, and the dynamical behavior is determined through solution of the circuit equations. Thus the system is described by ordinary differential equations, rather then the partial differential equations of the usual magnetohydrodynamic treatment.

The principal difficulty in this approach lies in determining the inductances. These change as the geometry of the beam and liner changes, and have to be recalculated at every timestep. Unless some approximation is invoked to simplify them, no computational advantage results from the circuit theory technique. Fortunately, such an approximation is available in many charged-particle ring configurations of interest, namely that of large aspect ratio. That is, the major radius R_j of the j th current loop is taken to be large compared with its minor dimension and the separation in the $r-z$ plane between it and any other loop. It is not necessary but is often convenient to assume that resistance and current are distributed uniformly throughout the $r-z$ cross section of the loop. The latter may be of arbitrary shape, but is usually taken to be circular or rectangular.

In this conception, collisions between the ion beam and background plasma enter as a resistance (and possibly an Ohkawa current[6]). Plasma energy losses by radiation and convection also affect the beam dynamics through the inductances and the resistance. Consistent with this approach, the inertia of the various particle species is ignored (except in the centrifugal force), so that the beam and plasma remain in force balance with the wall currents.

The code described here was originally[1,7] developed for an ion-beam-plasma interaction problem related to but distinct from that of producing field reversal. We started with a ring of deuterium (D) ions assuming an already existing field-reversed geometry. The ring was compressed by implosion of the liner, and the thermonuclear energy production arising from collisions between the beam ions and T or He^3 target ions in the background plasma was studied. An attempt was made to balance the components of the system so that the collisional slowing-down of the beam ions just canceled their tendency to speed up because of angular momentum conservation. "Clamping" the beam in this way at the energy for which the beam-target reaction rate peaks ($\sim$150 keV for D-T reactions) maximizes Q, the ratio of the yield to the sum of liner and plasma energy. It was found however that even with optimized parameters, Q was limited to 10% or less. The reason was that the energy given up by beam ions in collisions, most of which went into electron heating, caused expansion of the toroidal beam-plasma system and reduced all of the number densities, and accordingly reduced the beam-target reaction rate. Presumably Q would increase if a method were found to cool the electrons and recycle their thermal energy.

Some results from this earlier work will be displayed for purposes of illustration, but the method is much more general in applicability. Instead of assuming a preexisting state of field reversal, one can employ the code to study its origin and development in time. This problem will not however, be addressed in the present paper, which is devoted to describing the code and some of the techniques employed in its implementation. The plan of the paper is as follows. In Section II we derive the equations of the circuit theory model of the beam-plasma-liner dynamical system. In Section III we discuss isentropic (lossless) compression of an ion ring and the role of the induced electron current in the resultant scaling. Collisions are described in Section IV. The implementation of conduction, particle transport processes and

other phenomena is discussed in Section V, and an example is described in Section VI. Our results are summarized in Section VII. A listing of the code is given in an Appendix.

II. LINER MOTION AND EQUIVALENT CIRCUIT EQUATIONS

It is natural to represent the ion beam (and the currents carried by the electrons and target ion) as a current loop. It is equally convenient, though perhaps less natural, to represent the axial current profile on the liner (and possibly on the driver coil) as a superposition of coaxial current loops. Each such loop constitutes an electrical circuit individually coupled to each of the others, and contains a self-inductance and a resistance (arising from charged-particle encounters in the case of the ring). The circuit elements vary in time as the geometry charges.

Thus it is possible to calculate the implosion dynamics to any desired degree of realism entirely by means of the equivalent circuit equations. This representation is, in fact, a type of "finite-element" simulation. The minimum number of such circuits required to describe electromagnetic implosions of the liner is one each for the driver, liner and ring. In this limit the equivalent circuit is that shown in Fig. 2.

The circuit equations take the form

$$\frac{d\Phi_j}{dt} = -\mathcal{R}_j I_j \tag{1}$$

where j runs over all current-carying loops in the system. For the circuit of Fig. 2, $j = d,l,r$ (signifying driver, liner, and ring, respectively). The flux threading the j th element is

$$\Phi_j = \sum_k \mathfrak{M}_{jk} I_k, \tag{2}$$

where $\mathfrak{M}_{jk}$ is the inductance coupling circuits j and k, and $\mathcal{R}_j$ is the resistance of the j th circuit. Equation (1) describes the evolution of Φ_j. Given a knowledge of the Φ_j and the induction coefficients $\mathfrak{M}_{jk}$, Eq. (2) then can be solved for the I_j by matrix inversion.

If the driver is static and energized only during the outermost portion of the cycle, we can make an additional simplification by restricting our attention to times when the liner and ring are far removed from the driver coil. Then j, k take on only the values l,r, and there are just two each of equations (1) and (2). The numerical results described and plotted below were obtained using this two-loop circuit. It should be clear, however, that most of the discussion which follows is independent of the number of loops employed. We have experienced no difficulty in implementing versions of the code where as many as ten loops are employed to simulate the current profile in the liner. It appears that it would be easy to generalize the method to multiple ion rings or single rings with multiple constituent current filaments.

The coefficients $\mathfrak{M}_{jk}$ are very easily calculated. Since the ring deforms freely, it tends to evolve so as to maximize its self-inductance, that is, toward a circular cross-section. Moreover, one wants to consider configurations where ring and liner are close together, to minimize the volume filled with magnetic energy. Thus all distances separating current-carrying filaments are small compared with the major radii R, R_l (Fig. 1). In this limit the self and mutual inductances can be calculated in the large-aspect-ratio approximation as

$$\mathfrak{L}, \mathfrak{M} \simeq \mu_o R\,[\ln(8R) - 2 - \ln\bar{D}], \tag{3}$$

where the average is over the current-carrying part of the cross section, and the minor diameter D satisfies $D \ll R$.

Using (3) we find that the self-inductance of the ring is given by

$$\mathfrak{L}_r \equiv \mathfrak{M}_{rr} = \mu_o R\,[\ln(8R/r) - 2 + \delta] \tag{4}$$

where r is the ring minor radius, and δ depends on the details of the assumed current profile. For example, if all the current is carried in a skin located at the minor radius, $\delta = 0$; if the current is uniformly distributed, $\delta = 0.25$; and if the ring looks like a Bennett pinch in cross-section, $\delta = 0.5$. Similarly, the self-inductance of a liner segment is approximately (assuming the current is carried on the inner surface)

$$\mathfrak{L}_l \equiv \mathfrak{M}_{ll} \simeq \mu_o R_l \left[\ln\left(\delta R/l\right) - 1/2\right] \tag{5}$$

where l is the length of the segment, assumed much larger then the thickness, and R_l is the inside radius; and

$$\mathfrak{M}_{lr} = \mu_o (RR_l)^{1/2} \left\{ \ln \left\{ \frac{8(RR_l)^{1/2}}{\left[(R-R_l)^2 + (l/2)^2\right]^{1/2}} \right\} - 1 \right.$$
$$\left. \left\{ - \left[(R_l - R)/(l/2)\right] \tan^{-1}\left[(l/2)/(R_l - R)\right] \right\} \right\} \tag{6}$$

More important than the exact forms of (5) and (6) (which depend on the cross sections assumed to describe the liner) is the fundamental geometrical requirement $M_{lr}^2 \leqslant L_r L_l$, with equality holding only if $R = R_l$. Since Eqs. (4-6) are approximate, this inequality must be enforced by means of an explicit interpolation; otherwise, the ring can pass right through the liner. The interpolation formula actually used is

$$\mathfrak{M}_{lr} = \mathfrak{M}_{lr} + \left[(\mathfrak{L}_r \mathfrak{L}_l)^{1/2} - \mathfrak{M}_{lr}\right] \left[1 + \left[(R_l - R)/r\right]^p\right], \tag{7}$$

where M' is the corrected value of the mutual inductance. The dynamical results are not very sensitive to the choice of p, which was taken to be 10 in the numerical calculation.

As is well known from electromagnetic theory, the force tending to change any coordinate θ on which an inductive coefficient $\mathfrak{M}_{jk}$ depends is given by

$$F_{jk} = - I_j I_k \frac{\partial \mathfrak{M}_{jk}}{\partial \theta}. \tag{8}$$

Employing (8) consistently with the definitions used for $\mathfrak{M}_{jk}$ guarantees conservation of total energy, the magnetic portion of which is

$$W_M = \frac{1}{2} \sum_{j,k} \mathfrak{M}_{jk} I_j I_k = \frac{1}{2} \sum_j I_j \Phi_j \tag{9}$$

Thus in carrying out numerical calculations, we determine the total force of the ring acting on the liner according to

$$F_l = - I_r \sum_j I_j \frac{\partial \mathfrak{M}_{rj}}{\partial R_l}, \tag{10}$$

where the summation runs over the ring and all segments of the liner; while the same expression with opposite sign yields the force with which the liner tends to hold the ring in place. The liner equation of motion is thus

$$M_l \ddot{R}_l = F_l \tag{11}$$

Similarly, the electromagnetic force acting to constrict the ring is given by Eq. (8) with $\theta = r$:

$$F_r = - I_r \sum_j I_j \frac{\partial \mathfrak{M}_{rj}}{\partial r}. \tag{12}$$

Most of the force F_r comes from the term containing $\mathfrak{M}_{rr} = \mathfrak{L}_r$. Because of the use of the interpolation formula, Eq. (7), however, there is a small contribution from the liner-ring mutual inductances.

III. ISENTROPIC COMPRESSION

It is possible to develop scaling laws in terms of which the liner motion and beam and plasma evolution are described by analytic expressions, provided we assume the absence of both fusion reactions and loss mechanisms. This model is not a useful starting point about which to perturb to describe a realistic reactor design, because the latter is quite sensitive to beam slowing and the heating resulting from production of charged fusion reaction products. It is, however, valuable in describing the dynamics in the absence of a target plasma, as well as guiding us in developing an intuition about the interdependence of various parts of the system.

If the liner is represented by J_l distinct current-carrying segments, there are $J_l + 1$ fluxes and $J_l + 11$ physical variables. In our numerical calculations we usually took $J_l = 1$. For this case the 12 physical quantities used to describe a dynamical state of the system are the fluxes Φ_l and Φ_r linking the liner and ring, respectively; R and R_l; the ring minor radius r; the total

numbers of beam and target ions, N_B and N_T, respectively; the beam, target and electron temperatures, T_B, T_T and T_e, respectively; and the mean azimuthal ion drift velocities v_B and v_T. To proceed, we write down all the conservation laws that are available. The conserved quantities are the magnetic flux threading the j th liner segment

$$\Phi_j = \sum_l \mathfrak{M}_{jl} I_l + \mathfrak{M}_{rj} = \Phi_j^o, \tag{13}$$

and that threading the ring,

$$\Phi_r = \mathfrak{L}_r I_r + \sum_l \mathfrak{M}_{rl} I_l = \Phi_r^o; \tag{14}$$

the specific angular momentum of beam ions,

$$R v_B = R^o v_B^o, \tag{15}$$

and of target ions,

$$R v_T = R^o v_T^o; \tag{16}$$

the total ion numbers for each species

$$N_B = N_B^o, \tag{17}$$

$$N_T = N_T^o; \tag{18}$$

and the beam, target and electron entropy functions:

$$T_B V^{\gamma-1} = T_B^o (V^o)^{\gamma-1}, \tag{19}$$

$$T_T V^{\gamma-1} = T_T^o (V^o)^{\gamma-1}, \tag{20}$$

$$T_e V^{\gamma-1} = T_e^o (V^o)^{\gamma-1}. \tag{21}$$

Here $V = 2\pi^2 R r^2$ is the volume of the beam/plasma ring. Superscripts (^{o}) indicate an initial or a reference state of the system (e.g., the state of maximum compression). To these equations must be added the condition of force balance on the ring in the direction of major and minor radius,

$$0 = I_r \sum_l I_l \frac{\partial \dot{\mathfrak{M}}_{rl}}{\partial R} + \frac{1}{2} I_r^2 \frac{\partial \mathfrak{L}_r}{\partial R} + p \frac{\partial V}{\partial R} + \frac{N_B m_B v_B^2}{R} + \frac{N_T m_T v_T^2}{R} \tag{22}$$

and

$$0 = \frac{1}{2} I_r^2 \frac{\partial \mathfrak{L}_r}{\partial r} + I_r \sum_l I_l \frac{\partial \mathfrak{M}_{rl}}{\partial r} + p \frac{\partial V}{\partial r}, \tag{23}$$

respectively. Here $p = k[N_B T_B + N_T T_T + N_e T_e] V^{-1}$ is the internal pressure in the ring (k is the Boltzmann constant), and the electron number is obtained from the condition of charge neutrality,

$$N_e = N_B Z_B + N_T Z_T, \tag{24}$$

where Z_α is the charge state of ion species α. The last two terms in eq. (22) are the centrifugal force terms derived from the circulation of the respective species; that corresponding to the target ions is usually negligible.

Equations (22) and (23) have been derived assuming that the ring inertia is negligible, i.e., that the ring repositions itself instantaneously in response to any change in the position of the liner. In addition, the electron mass has been set to zero systematically, as negligible in comparison with those of the ions. The ring current I_r satisfies

$$I_r = I_B + I_T + I_e, \tag{25}$$

where

$$I_B = \frac{N_B e Z_B v_B}{2\pi R}, \tag{26}$$

$$I_T = \frac{N_T e Z_T v_T}{2\pi R}, \tag{27}$$

and

$$I_e = -\frac{N_e e v_e}{2\pi R}. \tag{28}$$

Equations (1), (11) and (13-23) contribute a set of $12 + J_l$ fundamental algebraic equations in terms of the $12 + J_l$ physical quantities defining the state. [All the others are expressible in terms of these through Eqs. (2), (4-6), and (24-28).] Thus, specifying the state variables determines the evolution of the system completely. We rewrite the liner force equation as

$$\frac{d}{dt}(R_l\dot{R}_l) = \left\{R_l^2\dot{R}_l^2(R_l^{-2} - R_l'^{-2}) + \sum_l \left[\frac{1}{2}I_l^2\frac{\partial \mathfrak{L}_l}{\partial R_l} + I_l I_r \frac{\partial \mathfrak{M}_{rl}}{\partial R_l}\right]/(2\rho L R_l)\right\}/\ln(R_l'^2/R_l^2)$$

which parametrizes the dynamical history in terms of t. Equation (29) is derived by assuming conservation of the liner mass $M_l = 2\pi\rho L\ (R_l'^2 - R_l^2)$; ρ is the (uniform) liner density, L is the overall length, and R_l' is the outer liner radius.

Let us assume now that the electron current tending to neutralize I_B is zero. Then by conservation of angular momentum,

$$I_r = \frac{e}{2\pi R}\ (N_D v_D + N_T v_T) = \frac{e}{2\pi R^2}\ (N_D R v_D + N_T R v_T) \sim R^{-2}. \tag{30}$$

The minor radius force balance condition (23) reduces to

$$p = \frac{\mu_o}{4}\frac{RI_r^2}{V} \sim r^{-2}R^{-4} \tag{31}$$

Equations (19-21), weighted by the respective total numbers N_j, sum to the adiabatic law

$$pV^\gamma = \text{const.} \tag{32}$$

Taking $\gamma = 5/3$ and combining (31) and (32) yields

$$r \sim R^{7/4} \tag{33}$$

Hence the number densities for species $\alpha(\alpha = B,\ T,\ e)$, $n_\alpha = N_\alpha/V$, satisfy

$$n_\alpha \sim V^{-1} \sim R^{-9/2}, \tag{34}$$

and the poloidal field near the ring $B_p = \mu_o I_r/2\pi r$ satisfies

$$B_p^2 \sim p \sim R^{-15/2} \tag{35}$$

We thus have a situation in which almost three-dimensional compression of the ring occurs as $R \simeq R_l$ is reduced. The poloidal field (35) rises almost as the inverse fourth power of R and the temperatures scale like $T \sim R^{-3}$.

At the other extreme, the motion of the liner may be such as to induce electron currents I_e totally neutralizing the change in ion current,

$$I_r \approx \text{const} \tag{36}$$

Going through the same steps as above, we find

$$r \sim R^{-5/4} \tag{37}$$

and hence

$$n_\alpha \sim V^{-1} \sim R^{3/2}, \tag{38}$$

and

$$B_p^2 \sim p \sim R^{5/2}. \tag{39}$$

In this limit the beam/plasma system *decompresses* during implosion, with n, p and B_p decreasing.

The actual result obtained by numerical solution of the equations naturally lies between these two extremes. The ring is always observed to compress, but at a rate slower then that given by Eqs. (34-35), and the scaling is not a power law in R. If $I_e = 0$ initially, the behavior tends to resemble the second model increasingly as turnaround is approached. The dependence of the degree of field reversal on the magnitude of the electron current induced during compression[5] explains why attempts to derive a scaling law for this parameter[3,8] do not appear to yield a simple result. There is, in fact no clear-cut way to predict the scaling without specifying the geometry of the compression.

IV. COLLISIONS

The electron thermal spread is assumed to be much larger than the thermal spread of either ion distribution or the relative drift between any two species. The average momentum transfer rate resulting from a collision between particles of species α and β is given by

$$m_\alpha \left[\frac{d\mathbf{v}_\alpha}{dt}\right]_\beta = -\nu_S^{\alpha/\beta} m_\alpha (\mathbf{v}_\alpha - \mathbf{v}_\beta) \tag{40}$$

where

$$\nu_s^{B/T} = \frac{4\pi Z_B^2 Z_T^2 e^4 (1 + m_B/m_T) \ln \Lambda \; n_T}{m_B^2 \; V_{BT}^3}; \tag{41}$$

$$\nu_s^{\alpha/e} = \frac{4\sqrt{2\pi}}{3} \frac{Z_\alpha^2 e^4 (1+m_\alpha/m_e) m_e^{3/2} n_e \ln \Lambda}{m_\alpha^2 (kT_e)^{3/2}}, \tag{42}$$

$\alpha = B,T$, and, from conservation of momentum,

$$n_\alpha m_\alpha \nu_s^{\alpha/\beta} = n_\beta m_\beta \nu_s^{\beta/\alpha} \tag{43}$$

Here $\ln \Lambda$ is the form of the usual Coulomb logarithm appropriate to the species pair α, β, and $v_{\alpha\beta} = |v_\alpha - v_\beta|$. Correspondingly, the average temperature rate of change resulting from a collision is.

$$k\left(\frac{dT_B}{dt}\right)_T = \frac{8\pi}{3} \frac{Z_B^2 Z_T^2 e^4}{m_B} \frac{n_T \ln \Lambda}{V_{BT}}; \tag{44}$$

$$k\left(\frac{dT_T}{dt}\right)_B = \frac{8\pi}{3} \frac{Z_B^2 Z_T^2 e^4}{m_T} \frac{n_B \ln \Lambda}{V_{BT}}, \tag{45}$$

for ion-ion encounters, and

$$k\left(\frac{dT_\alpha}{dt}\right)_e = \frac{8\sqrt{2\pi}}{3} \frac{Z_\alpha^2 e^4 \sqrt{m_e}\, n_e \ln \Lambda}{m_\alpha (kT_e)^{3/2}} k(T_e - T_\alpha), \tag{46}$$

$\alpha = B,T$, for ion-electron encounters, with the remaining rates $(dT_e/dt)_\alpha$ defined so as to satisfy conservation of energy.

Consideration of the magnitudes of these rate formulas reveals the following general features: (*i*) both electron and target ions contribute significantly to the rate at which beam ions slow down; (*ii*) the *relative* velocity with which beam ions move with respect to the target ions is chiefly affected by $B-T$ collisions, because electron collisions act in the same sense (as a drag) on both ion species; (*iii*) thermalization of the beam also results principally from collisions with target ions.

On the basis of these generalizations, we can estimate the relative slowing down of beam and target ions through collisions as

$$\frac{d}{dt}(v_B - v_T)_{\text{coll}} \simeq -(\nu_s^{B/T} - \nu_s^{T/B})(v_B - v_T) \tag{47}$$
$$\equiv -\nu_s (v_B - v_T).$$

For the usual case where the target ion mass density substantially exceeds that of the beam, $n_T m_T >> n_B m_B$, Eq. (47) implies

$$\nu_s \simeq \nu_s^{B/T}. \tag{48}$$

at the same time, the adiabatic compression produced by the imploding liner tends to cause both ion species to accelerate in the azimuthal direction according to

$$\left(\frac{dv_\alpha}{dt}\right)_{\text{adiab}} = - v_\alpha \frac{\dot{R}}{R} \simeq - v_\alpha \frac{\dot{R}_l}{R_l} \tag{49}$$

Taking the difference between the beam and target equation (49) yields

$$\frac{d}{dt} (v_B - v_T)_{\text{Adiab}} \simeq - \frac{\dot{R}_l}{R_l} (v_B - v_T). \tag{50}$$

Eqs. (47 and (50) give for the net time rate of change of the relative velocity

$$\frac{d}{dt} (v_B - v_T) \simeq - (\dot{R}_l/R_l + \nu_s) (v_B - v_T) \tag{51}$$

The condition that this relative velocity be a constant is thus

$$\dot{R}_l/R_l = - \nu_s \tag{52}$$

When Eq. (57) is satisfied, the beam is said to be *clamped*[10]. With a tritium target there is an advantage in clamping the beam at a relative energy $\epsilon = \frac{1}{2} m_B v_{BT}^2 \sim 150$ keV which maximizes the reaction rate for D-T fusion.

Clamping is of course accompanied by a monotonic increase in thermal energy according to Eqs. (44-45). The ion thermal energy density $w'_{th} = \frac{3}{2} k(n_B T_B + n_T T_T)$ increases as a result of ion-ion collisions at a rate

$$\frac{dw'_{th}}{dt} = \frac{4\pi Z_B^2 Z_T^2 e^4 n_B n_T \ln\Lambda}{v_{BT}} \left(\frac{1}{m_B} + \frac{1}{m_T}\right) \tag{53}$$

$$= \nu_s^{B/T} n_B m_B v_{BT}^2$$

Using (48), we see by comparison of (52) and (53) that the time scale for implosions of the liner is comparable to that for heating up the ion beams. The electron heating rate can be even faster.

Note that if ν_s were approximately constant, the clamping condition (52) would imply an exponential decrease in R_f with time. As this is not realizable, clamping evidently cannot be maintained close to turnaround.

In differencing the equations in the code, we found it convenient to use as dependent variables quantities that are approximately conserved. Thus instead of T_α we used the entropy functions [Eqs. (19-21)], which now satisfy equations of the form

$$\frac{d}{dt}\,(T_\alpha V^{\gamma-1}) = V^{\gamma-1} \sum_\beta \nu_T^{\alpha/\beta}\,(T_\beta - T_\alpha), \tag{54}$$

where the $\nu_T^{\alpha/\beta}$ are defined as the rates in Eqs. (44-46). Similarly, the slowing-down rates enter as

$$\frac{d}{dt}\,(R\mathrm{v}_\alpha) = R \sum_\beta \nu_s^{\alpha/\beta}(\mathrm{v}_\beta - \mathrm{v}_\alpha). \tag{55}$$

V. OTHER DISSIPATIVE PROCESSES

Collisions, discussed in section IV, can transform directed energy into thermal energy. Although essential for clamping, they may be deleterious if they (i) increase the ratio of beam ion gyroradius to ring thickness excessively; (ii) cause too much of the liner energy to go into pumping up the target plasma; or (iii) lead to premature loss of confinement as a result of decrease of beam current below that needed for field reversal. In addition, the following loss processes can remove energy from the system entirely: radiation, heat conduction along field lines, particle diffusion across lines, charge exchange with impurities, and ohmic heating within the liner. The last of these can have a second, more serious consequence: finite resistivity gives rise to diffusion of field lines through the liner, untrapping the magnetic flux which holds the ring at a safe distance from the liner.

Radiation processes are modeled by adding loss terms to the expression (55) for the time rate of change of the electron entropy function. For bremsstrahlung and synchrotron (cyclotron) radiation we have the terms

$$\frac{d}{dr}\left(V^{\gamma-1}\,T_e\right)_{br} = -\,V^{\gamma-1}\times\,5.35\times10^{-24}\,(N_D + N_T Z_T^2)\,T_e^{1/2} \tag{56}$$

and

$$\frac{d}{dt}\,(V^{\gamma-1}T_e)_{cyc} = -\,V^{\gamma-1}\times\,3.98\times10^{-16}\,\frac{\beta^2\bar{B}_p^2}{1-\beta^2}, \tag{57}$$

where T is given in eV, $\beta^2 = \frac{3}{2}\,kT_e/m_ec^2$ and $B_p = \mu_o I_r/2\pi r$. In the spirit of the circuit-theoretical approach (wherein the ring is a macroscopic circuit element with certain lumped parameters derived from microscopic processes), the radiation rates are calculated by averaging the field strength over the ring cross-section.

In the same fashion, thermal conduction losses can be treated by writing

$$\frac{d}{dt}\left(V^{\gamma-1}\,T_\alpha\right)_{cond} = -\,V^{\gamma-1}\,4\pi^2 Rr\,\kappa_\alpha\,(T_\alpha/r) = -\,V^{\gamma-1}\,4\pi R\,\kappa_\alpha T_\alpha, \tag{58}$$

where κ_α is the average cross field thermal conduction of species α. The fastest thermal loss process is that associated with the target ions, $\alpha = T$. Furthermore, thermal equilibration, alpha-particle heating, etc., can be included in an average sense in the same form.

Finally, particle losses can be estimated simply by assuming smeared-out density profiles according to some law like the Bennett pinch. If a given profile extends past the position of the separatrix, located at average minor radius $r = r_s$, that portion of the particles located at $r > r_s$ is lost. A simple calculation then gives the loss rate as the rate at which particles "fall over the edge." Thus we find

$$\left(\frac{dN_\alpha}{dt}\right)_{diff} = -\,\frac{Gr^2}{r_S^2}\,\nu_s^\alpha N_\alpha, \tag{59}$$

where G is a geometrical factor (equal to 12 for a Bennett profile) which decreases as the assumed profile becomes more localized, and ν_s^α is the total scattering rate for species α.

VI. A NUMERICAL EXAMPLE

Using the equations and techniques described in Section II-V, we consider the following situation. A liquid lithium liner (density $\rho = 0.54$ g/cm^3) of length $L = 13.5$ cm and inner and

outer radii 31.59 cm and 48.43 cm implodes with velocity 3×10^4 cm/s on a fully ionized D-He^3 ring with major and minor radii of 30 cm and 0.758 cm, respectively. The initial target ion number densities are $n_{He^3} = 2n_D = 3.59 \times 10^{16}\,\mathrm{cm}^{-3}$. The temperatures are $T_D = 23.7$ keV, $T_{He^3} = 1$ keV and $T_e = 10$ keV. The deuterium current is 1.52 MA, twice the electron back current. These numbers are chosen to give a beam ion streaming energy of 550 keV and a poloidal field of 200 kG, with beam clamping. Since the emphasis was on determining Q, only the part of the evolution in the vicinity of liner turnaround was considered, and the early-time conditions giving rise to these parameters were not investigated.

Figure 3 shows how the beam and liner radii change in time. Note that the separation increases, a reflection of the increase in beam minor radius (Fig. 4). Correspondingly the number densities (Fig. 5) drop, level off as collisional heating and compression come into balance, then drop again in the expansion (decompression) stage, and the poloidal field (Fig. 6) decreases, increases, then decreases monotonically after turnaround. The various forms of energy (magnetic, liner kinetic, ion directed, and thermal) are plotted in Fig. 7, along with the fusion yield. Figure 8 shows how the component temperatures increase near turnaround, the evident irreversibility being a consequence of collisions.

Running time on the calculation using an IBM 360/168 was 91 seconds, of which about a quarter was required for diagnostics. Using ten current loops to represent the liner current profile approximately doubles the running time, since roughly twice as many differential equations have to be solved [matrix inversion of Eq. (2) does not add any substantial amount to the total]. It turns out to be convenient in writing the code to make extensive use of nested sequences of statement functions in redetermining force balance on each time step, and most of the running time is expended in this task.

A variety of prescriptions are possible for defining the initial conditions. The main thing is to insure that they be neither over- nor underdetermined. When working with multiple liner

current loops, we arbitrarily imposed the condition that the flux threading all the loops be the same. Though straightforward, this is unlikely to be a good approximation in the late stages of the implosion if finite liner resistivity is modeled.

VII. CONCLUSIONS

We have presented a new numerical technique for solving problems involving the dynamics of charged particle rings. Its principle advantage is that it is couched in circuit-theoretical terms, obviating the need for solution of partial differential equations. Because of its adaptation to the physics and geometry of such problems, the method can be implemented with only a small number ($\sim$ 10) of current carrying elements. In effect, it replaces the uniform or quasi-uniform mesh of the standard 2D finite-difference technique with a highly nonuniform "mesh" of circuit elements, located optimally to reflect the relevant physics.

The code has been applied to calculations of the thermonuclear yield and other characteristics of a beam-target fusion device. The particular concept for which the code was originally developed turns out to be disappointing in terms of its efficiency as a reactor (the examples of Section VI yielded $Q \approx 3.2\%$), and also appears to be unstable to kink modes[11]; however it may have non-fusion applications. It is clear that the code can be applied to a variety of axisymmetric situations involving field reversal and changes of system geometry, and therefore is potentially of wider utility.

This work was supported by the Office of Naval Research.

References

1. P. Dreike, R. L. Ferch, A. Friedman, S. Humphries, R. V. Lovelace, G. Ludwig, R. N. Sudan, D. L. Book, G. Cooperstein, A. T. Drobot, J. Golden, S. A. Goldstein, C. A. Kapetanakos, R. Lee, W. Manheimer, S. J. Marsh, D. Mosher, E. Ott, S. S. Stephanakis,

and P. J. Turchi, *Plasma Physics and Controlled Nuclear Fusion Research 1976* (IAEA, Vienna, 1977), v. 3, p. 415.

2. S. J. Marsh, A. T. Drobot, J. Golden and C. A. Kapetanakos, *Phys. Res. Lett.* **39**, 705 (1977).

3. R. N. Sudan and E. Ott, *Phys. Rev. Lett.* **33**, 355 (1974).

4. D. E. Baldwin and T. K. Fowler, Lawrence Livermore Laboratory Rept. UCID-17691 (1977).

5. D. E. Baldwin and M. E. Rensink, Lawrence Livermore Laboratory Rept. No. (submitted to *Phys. Rev. Lett.*).

6. T. Ohkawa, Nuclear Fusion **10**, 185 (1970).

7. D. L. Book and P. J. Turchi, Bull. APS **20**, 1278 (1975). Abstract

8. E. S. Weibel, Phys. Fluids **20**, 1195 (1977).

9. S. I. Braginskii, *Reviews of Plasma Physics*, vol. 1 (Consultants Bureau, New York, 1965), p. 205.

10. 10. J. M. Dawson, H. P. Furth and F. H. Tenney, *Phys. Rev. Lett.* **26**, 1156 (1971).

11. R. N. Sudan and M. N. Rosenbluth, *Phys. Rev. Lett.* **36**, 972 (1976); R. N. Sudan and M. N. Rosenbluth (to be published).

```
C
C     "ION BEAM-PLASMA INTERACTION CLAMPED THROUGH AXIAL COMPRESSION"
C
C     THIS PROGRAM CALCULATES COMPRESSION, HEATING AND BURN IN AN AXIALLY
C     COMPRESSED BEAM-TARGET PLASMA.  THE BEAM IS A RING OF D IONS, THE
C     TARGET A MIXTURE OF COLD TRITIUM AND HOT ELECTRONS.  THE CONFINING
C     MAGNETIC FIELD BUILDS UP OWING TO COMPRESSION PRODUCED BY AN
C     IMPLODING LITHIUM LINER (LINUS), DRIVEN ELCTROMAGNETICALLY BY
C     EXTERNAL THETA-PINCH WINDINGS.  PARAMETERS ARE CHOSEN SO THAT
C     COMPRESSION, COLLISIONAL SLOWING OF THE D BEAM, AND LOSSES BALANCE,
C     PRODUCING A SITUATION IN WHICH THE BEAM IS CLAMPED FOR THE ENTIRE
C     DURATION OF THE COMPRESSION.
C     D. L. BOOK, P. J. TURCHI & D. L. STEIN
C
      IMPLICIT REAL*8 (A-I, K-Z), INTEGER*4 (J), REAL*4 (S)
      LOGICAL*4 COLL, LOSS, BURN, FORWRD
      COMMON/ NEWTON/ DT0,JITER
      COMMON /QBLOCK/ Q(25)
      COMMON/ ARRAY/ Y(25), DY(25), Y0(25)
      EXTERNAL DERIV
      NAMELIST /LINER/ R10, R20, RW, B20, RH0, OMEGA, LNGTH0, ETA,
     1     SPHT, TL, PCA
      DATA R10, R20, RW, B20, RH0, OMEGA, LNGTH0, ETA, SPHT, TL, PCA
     1     / 2.06D2, 2.126D2, 3.D2, 0.D0, .54D0, 0.D0, 13.5D0,
     2     45.2D-7, 6.D7, 5.D2, .1D0 /
      NAMELIST /PLASMA/ RMAJOR, WD, TD, TE, TT, BP, VRATIO, NRATIO,
     1     IRATIO
      DATA RMAJOR, WD, TD, TE, TT, BP, VRATIO, NRATIO, IRATIO /
     1     2.D2, 7.D2, 1.D2, 1.D2, 1.D2, 5.D5, .5D0, 1.D0, .5D0 /
      NAMELIST /LOGICL/ COLL, LOSS, BURN, FORWRD
      DATA COLL, LOSS, BURN, FORWRD / .TRUE., .TRUE., .TRUE.,
     1     .FALSE. /
      NAMELIST /CNTROL/ DT, DTPLOT, DTFILM, DTDUMP, TLAST, T, TPLOT,
     1     TFILM, TDUMP
      DATA DT, DTPLOT, DTFILM, DTDUMP, TLAST, T, TPLOT, TFILM, TDUMP
     1     /1.D-5, 1.D-4, 1.D-3, 1.D-2, .100, 0.D0, -1.D-12, -1.D-12,
     1     -1.D-12 /
      CALL INDUMP
      CALL CRDUMP(40,10)
C
C     INITIALIZE.
C
 10   READ (5,LINER,END=100)
      READ (5,PLASMA,END=100)
      READ (5,LOGICL,END=100)
      READ (5,CNTROL,END=100)
      PRINT 98
      DO 11  J = 1, 5
 11   PRINT 99
      WRITE (6,LINER)
      WRITE (6,PLASMA)
      WRITE (6,LOGICL)
      WRITE (6,CNTROL)
      DO 15  J = 1, 25
 15   Q(J) = 0.D0
      JITER=0
      DTMAX = DT
      DT0=DT
      CALL INPUT(T,
     1     R10, R20, RW, B20, RH0, OMEGA, LNGTH0, ETA, SPHT, TL, PCA,
     2     RMAJOR, WD, TD, TE, TT, BP, VRATIO, NRATIO, IRATIO,
     3     COLL, LOSS, BURN, FORWRD,
T20827    DTPLOT, DTFILM, DTDUMP, TLAST, TPLOT, TFILM, TDUMP)
```

```
C
C     PERFORM DUMPS, DIAGNOSTICS AT APPROPRIATE INTERVALS.
C
  20      IF (T .LT. TDUMP)  GO TO 30
          TDUMP = TDUMP + DTDUMP
  30      IF (T .LT. TFILM)  GO TO 40
          TFILM = TFILM + DTFILM
  40      IF (T .LT. TPLOT)  GO TO 50
          TPLOT = TPLOT + DTPLOT
          CALL DERIV(T,JTOTAL)
          IF (T .EQ. 0.D0)  PRINT 90
          IF (T .NE. 0.D0)  PRINT 91, T
          DATA SY, SY0, SDY, SLI, SRING, SPLAS, SNU, SCNU, SDATA /
     1         'Y   ', 'Y0  ', 'DY  ', 'LI  ', 'RING', 'PLAS', 'NU  ',
     2         'CNU ', 'DATA' /
          CALL DSPLAY(SY)
          CALL DSPLAY(SY0)
          CALL DSPLAY(SDY)
          CALL DSPLAY(SLI)
          CALL DSPLAY(SRING)
          CALL DSPLAY(SPLAS)
          CALL DSPLAY(SNU)
          IF ( T .GT. 0.D0)  GO TO 50
          CALL DSPLAY(SCNU)
          CALL DSPLAY(SDATA)
  50      CONTINUE
C
C     ADVANCE VARIABLES ONE TIMESTEP.
C
          JITER=0
          IF (Y(3) .NE. 0.D0)  DT = DMIN1(DTMAX, .05D0*DABS(Y(2)/Y(3)))
          DT0=DT
          CALL INT(JTOTAL,T,DERIV,DT)
          IF (T .LT. TLAST)  GO TO 20
          GO TO 10
  90      FORMAT('0', 'INITIAL DISPLAY, INCLUDING TABULATED CONSTANTS:')
  91      FORMAT('1', 'DISPLAY AT TIME T = ', 1PD10.4, ' SEC:')
  98      FORMAT('1', 60X, 'I P I C A C' // ' ', 35X, 'ION BEAM-',
     1         'PLASMA INTERACTION CLAMPED THROUGH AXIAL COMPRESSION')
  99      FORMAT('+', 35X,                              'I          ',
     1         'P       I           C                A     C          ')
 100      RETURN
          E N D
C
      SUBROUTINE DERIV(TIME,JTOTAL)
          IMPLICIT REAL*8 (A-I, K-Z), INTEGER*4 (J), REAL*4 (S)
          INTEGER*4 MOD
          DIMENSION RLINER(5), EMAG1(5)
          DIMENSION ZA(3,3), ZR(3)
          DIMENSION RMAJ1(4),RMAJ2(4),RMIN1(4),RMIN2(4)
          COMMON / NEWTON /DT, JITER
          COMMON / INCB / MU, KMU
          COMMON/ RADII/ RMINOR,RMAJOR,RJ
          COMMON / PBLOCK / P
          COMMON/ COEFF/ KCF,NDTOT, RVD
          COMMON / CURREN / ILINER(3)
          COMMON/ LENGTH/  LNGTH(5), LHL8Q(5)
          COMMON / INDEX / JMAX, JMAX1
          COMMON/ FLUX/ PHI,PSI1(5)
          COMMON/ ARRAY/ Y(25), DY(25), Y0(25)
          LOGICAL*4 NOCOLL, NOLOSS, NOBURN,FORWRD
          DIMENSION $LINE(33)
C
C     THE FOLLOWING STATEMENT FUNCTIONS ARE USED BELOW IN SOLVING FOR
C     RMAJOR AND RMINOR BY REQUIRING THAT THE FORCES IN THE CORRESPONDING
C     DIRECTIONS VANISH.  HERE A, B, C ARE RESPECTIVELY THE MINOR AND
C     MAJOR RADII OF THE RING AND THE LINER INSIDE RADIUS, ALL IN CM.
```

```
C
      LR(A,B) = KMU*B*(DLOG(8.D0*B/A) - 2.D0 + KD)
      DALR(A,B) = -KMU*B/A
      DBLR(A,B) = KMU*(DLOG(8.D0*B/A) - 1.D0 + KD)
      LL(C,D)=MU*C*(DLOG(16.D0*C/D) - 0.5D0)
      DCLL(C,D)=MU*(DLOG(16.D0*C/D) + 0.5D0)
      LN(D,F)=0.5D0*(D/F)*DLOG(D)
      FAC(D,F)=(((F-D)**2)/(2.D0*D*F))*DLOG(DABS(F-D))
      MLL(C,D,F)=MU*C*(DLOG(16.D0*C)-LN(D,F)-LN(F,D)+FAC(D,F)-0.5D0)
      DCMLL(C,D,F)=MU*(DLOG(16.D0*C)-LN(D,F)-LN(F,D)+FAC(D,F)+0.5D0)
      MLR(B,C,F)=MU*DSQRT(B*C)*(.5D0*DLOG(6.4D1*B*C/((B-C)**2 +
     1     F)) - 1.D0 - ((B-C)/DSQRT(F))*DATAN(DSQRT(F)/(B-C)))
      DBMLR(B,C,F)=.5D0*MU*DSQRT(C/B)*(.5D0*DLOG(6.4D1*B*C/((B-C)**2
     1     +F))+((C-3.D0*B)/DSQRT(F))*DATAN(DSQRT(F)/(B-C)))
      DCMLR(B,C,F)=.5D0*MU*DSQRT(B/C)*(.5D0*DLOG(6.4D1*B*C/((B-C)**2
     1     +F))+((3.D0*C-B)/DSQRT(F))*DATAN(DSQRT(F)/(B-C)))
      MLRS(A,B,C,D,F)=MLR(B,C,F)+(DSQRT(LR(A,B)*LL(C,D))-MLR(B,C,F))
     1     /(1.D0+((C-B)/A)**P)
      DAMLRS(A,B,C,D,F)=(.5D0*DALR(A,B)*DSQRT(LL(C,D)/LR(A,B))+(P/A)
     1    *((C-B)/A)**P*(DSQRT(LR(A,B)*LL(C,D))-MLR(B,C,F))/(1.D0+
     2     ((C-B)/A)**P))/(1.D0 + ((C-B)/A)**P)
      DBMLRS(A,B,C,D,F)=DBMLR(B,C,F)+(.5D0*DBLR(A,B)*DSQRT(LL(C,D)/
     1     LR(A,B)) + (P/(C-B))*((C-B)/A)**P*(DSQRT(LR(A,B)*LL(C,D))-
     2    MLR(B,C,F))/(1.D0 + ((C-B)/A)**P))/(1.D0 + ((C-B)/A)**P)
      DCMLRS(A,B,C,D,F)=DCMLR(B,C,F)+(.5D0*DCLL(C,D)*DSQRT(LR(A,B)/
     1     LL(C,D))-(P/(C-B))*((C-B)/A)**P*(DSQRT(LR(A,B  )*LL(C,D))-
     2    MLR(B,C,F))/(1.D0 + ((C-B)/A)**P))/(1.D0 + ((C-B)/A)**P)
      NKT(A,B) = PVG/(KVOL*A*A*B)**GM1
      SIGMA(E) = 1.D-24*(A5 + A2/(1.D0 + (A3*E - A4)**2))/(E*
     1     (DEXP(A1/DSQRT(E)) - 1.D0))
      DATA ETOT0 / 0.D0 /
C
C     TIME (INDEPENDENT VARIABLE) HAS UNIT DERIVATIVE.
C
      DY(1) = 1.D0
C
C     REPLACE SUBSCRIPTED QUANTITIES WITH MORE FAMILIAR NOTATION.
C
      R1SQ = Y(2)
      RU = Y(3)
      PSI2 = Y(5)
      RVD = Y(7)
      RVT = Y(8)
      TDVGM1 = Y(9)
      TEVGM1 = Y(10)
      TTVGM1 = Y(11)
      NDTOT = Y(12)
      NTTOT = Y(13)
      EOHMIC = Y(14)
      ERAD = Y(15)
      NCOUNT = Y(16)
      PVGPRD = Y(17)
      BURNUP = Y(18)
      DO  5 J=1,JMAX1
5     PSI1(J)=Y(19+J)
      PHI=Y(19+JMAX)
C
C     FIND SOME OF THE QUANTITIES NEEDED TO DESCRIBE THE LINER DYNAMICS.
C
      R0SQ = RU*RU
      R2SQ = R1SQ + R0SQ
      R1 = DSQRT(R1SQ)
      R2 = DSQRT(R2SQ)
      U1 = RU/R1
      U2 = RU/R2
```

```
      B1 = KFLUX*PSI1(1)/R1SQ
      B2 = KFLUX*PSI2/(RWSQ - R2SQ)
      RLOG = DLOG(R2SQ/R1SQ)
      DRSQ = R1OSQ - R1SQ
      R12SQ = 1.D0/R1SQ - 1.D0/R2SQ
      PMAG1 = KP*B1*B1
      PMAG2 = KP*B2*B2
      U1BYR1 = U1/R1
C
C     NOW DO ION RING DYNAMICS AND PLASMA PROCESSES.  USE ALL THE
C     AVAILABLE ALGEBRAIC RELATIONS BEFORE COMPUTING ANY DERIVATIVES.
C     THE RING MAJOR AND MINOR RADII ARE FOUND USING NEWTON'S METHOD TO
C     SOLVE THE EQUATIONS FOR FORCE BALANCE IN THE RING, GIVEN THE FLUXES
C     WHICH ARE ENCLOSED BY THE RING AND LINER (PHI AND PSI1,
C     RESPECTIVELY), AND USING HANDBOOK FORMULAS FOR SELF- AND MUTUAL
C     INDUCTANCES.  MKS UNITS ARE USED IN THIS PORTION OF THE CODE.
C
C     EXTRAPOLATE FROM LAST TWO TIME STEPS TO GET GOOD INTIIAL GUESSES
C     FOR RMAJOR, RMINOR (USED ONLY ON EVEN STEPS OF R-K-G).
C
      IF (JITER .NE. 0)  GO TO 1
      JSTEP = 0
      DTOLD = DTNEW
      DTNEW = DT
      WT1 = -DTNEW/DTOLD
      WT2 = 1.D0 - WT1
    1 CONTINUE
C
      JSTEP = JSTEP + 1
      IF (MOD(JSTEP,2) .NE. 0)  GO TO 2
      RMAJOR = WT1*RMAJ1(JSTEP) + WT2*RMAJ2(JSTEP)
      RMINOR = WT1*RMIN1(JSTEP) + WT2*RMIN2(JSTEP)
    2 CONTINUE
C
      JIT = 0
      A = RMINOR
      B = RMAJOR
      RJ = R1
      PVG = KNKT*(NDTOT*(TDVGM1 + ZD*TEVGM1) + NTTOT*(TTVGM1 +
     1     ZT*TEVGM1)) + 1.D-7*PVGPRD
   10 CONTINUE
      DAFA=(FA(A+0/2.D0,B,RJ,NKT(A+0/2.D0,B))-FA (A-0/2.D0,B,RJ,
     1     NKT(A-0/2.D0,B)))/0
      DAFB=(FB(A+0/2.D0,B,RJ,NKT(A+0/2.D0,B))-FB (A-0/2.D0,B,RJ,
     1     NKT(A-0/2.D0,B)))/0
      DBFA=(FA(A,B+0/2.D0,RJ,NKT(A,B+0/2.D0))-FA(A,B-0/2.D0,RJ,
     1     NKT(A,B-0/2.D0)))/0
      DBFB=(FB(A,B+0/2.D0,RJ,NKT(A,B+0/2.D0))-FB(A,B-0/2.D0,RJ,
     1     NKT(A,B-0/2.D0)))/0
      DET = DAFA*DBFB - DAFB*DBFA
      FMINOR = FA(A,B,RJ,NKT(A,B))
      FMAJOR = FB(A,B,RJ,NKT(A,B))
      DA = (DBFB*FMINOR - DBFA*FMAJOR)/DET
      DB = (DAFA*FMAJOR - DAFB*FMINOR)/DET
      A = A - DA
      B = B - DB
      JIT=JIT+1
      IF (DABS(DB) .GT. RTEST*B .OR. DABS(DA) .GT. RTEST*A) GO TO 10
      RMINOR = A
      RMAJOR = B
      JITER=JITER+JIT
      ITER = DFLOAT(JITER)
      IF (MOD(JSTEP,2) .NE. 0)  GO TO 12
      RMAJ1(JSTEP) = RMAJ2(JSTEP)
      RMAJ2(JSTEP) = RMAJOR
      RMIN1(JSTEP) = RMIN2(JSTEP)
      RMIN2(JSTEP) = RMINOR
   12 CONTINUE
```

```
C
C     DEFINE THE FOLLOWING FOR DIAGNOSTIC PURPOSES.
C
          LL1=LL(RJ,LNGTH(1))
          LL2=LL(RJ,LNGTH(2))
          ML12=MLL(RJ,LNGTH(2),LNGTH(1))
          MLRS1=MLRS(RMINOR,RMAJOR,RJ,LNGTH(1),LHLSQ(1))
C
C     EVERYTHING ELSE CAN NOW BE CALCULATED.
C
          LRING = LR(RMINOR, RMAJOR)
          LLINER=LL(RJ,LNGTH(JMAX1))
          IRING=ILINER(JMAX)
          VD = RVD/RMAJOR
          VT = RVT/RMAJOR
          VOLUME = KVOL*RMAJOR*RMINOR**2
          ND = NDTOT/VOLUME
          NT = NTTOT/VOLUME
          NETOT = NDTOT*ZD + NTTOT*ZT
          NE = NETOT/VOLUME
          ID = KID*NDTOT*VD/RMAJOR
          IT = KIT*NTTOT*VT/RMAJOR
          IE = IRING - ID - IT
          VE = RMAJOR*IE/(KIE*NETOT)
C
C     HAVING COMPUTED THE MAGNETODYNAMIC PARAMETERS, WE CAN WRITE DOWN
C     THE EQUATIONS OF MOTION OF THE LINER.
C
          DY(2) = 2.D0*RU
          JMAX2=JMAX1-1
          FORCE=0.D0
          DO 14 J=1,JMAX1
          FORCE=FORCE+ILINER(J)*(0.5D0*ILINER(J)*DCLL(RJ,LNGTH(J))
     1         +IRING*DCMLRS(RMINOR,RMAJOR,RJ,LNGTH(J),LHLSQ(J)))
          IF(J.EQ.JMAX1)  GO TO 14
          JP1=J+1
          DO 13 JJ=JP1,JMAX1
13        FORCE=FORCE+ILINER(J)*ILINER(JJ)*DCMLL(RJ,LHLSQ(JJ),LHLSQ(J))
14        CONTINUE
          P1 = KF*FORCE/RJ
          P2 = PMAG2
          DY(3) = (RSQUSQ*R12SQ + OMEGA**2*(ROSQ + DRSQ*(2.D0*RLOG +
     1         DRSQ*R12SQ)) + 2.D0*(P1 - P2)/RHO)/RLOG
C
C     FIND TEMPERATURES FROM PRODUCT OF V TO POWER GAMMA - 1 AND T.
C
          VGM1 = VOLUME**GM1
          TD = TDVGM1/VGM1
          TE = TEVGM1/VGM1
          TT = TTVGM1/VGM1
C
C     KEEP TRACK OF RING, PLASMA ENERGETICS.
C
          EKIN = KKIN*RSQUSQ*RLOG
          EROT = KROT*(DRSQ**2*RLOG/2.D0 + ROSQ*(DRSQ + (R1SQ + R2SQ)/
     1         4.D0))
          EMAG2=LNGTH(JMAX1)*B2*B2*(RWSQ-R2SQ)/8.D0
          EMAG=0.5D7*IRING*PHI
          DO 16 J=1,JMAX1
          EMAGI(J)=0.5D7*ILINER(J)*PSII(J)
          EMAG=EMAG+EMAGI(J)
16        CONTINUE
```

```
            EMAG=EMAG+EMAG2
184077      WD = MD*VD**2/(2.D0*BOLTZ)
            WT = MT*VT**2/(2.D0*BOLTZ)
            EDDIR = NDTOT*BOLTZ*WD
            ETDIR = NTTOT*BOLTZ*WT
            EDTH = KE*NDTOT*TD
            ETTH = KE*NTTOT*TT
            EETH = KE*NETOT*TE
            EBEAM = EDDIR + EDTH
            EPLAS = ETDIR + ETTH + EETH
            ERING = EBEAM + EPLAS
            EPOT=ERING+EMAG
            ETOT = EKIN + EROT + EPOT
            IF (ETOT0 .EQ. 0.D0)  ETOT0 = ETOT
            YIELD = KYIELD*BURNUP
            Q = YIELD/ETOT0
            ENET = ETOT + ERAD + EOHMIC - YIELD
            PD = BOLTZ*ND*TD
            PE = BOLTZ*NE*TE
            PT = BOLTZ*NT*TT
            PTOT = PD + PE + PT
            BETA = KBETA*DSQRT(TE)
            BP = .2D0*IRING/RMINOR
            KAPPA = KPROP*VD/(RMINOR*BP)
            PPOL = KP*BP**2
            BETAPL = NKT(RMINOR, RMAJOR)/PPOL
            TL = EOHMIC/HTCAP + TL0
C
C     FIND ACCELERATION AT INNER, OUTER FACE OF LINER.
C
            O1 = OMEGA*R10SQ/R1SQ
            O2 = OMEGA*R20SQ/R2SQ
            G1 = (DY(3) - U1*U1)/R1 - O1*O1*R1
            G2 = (DY(3) - U2*U2)/R2 - O2*O2*R2
C
C     ZERO DERIVATIVES OF ION RING AND PLASMA QUANTITIES CONSERVED IN
C     THE ABSENCE OF DISSIPATION.
C
            JTOTAL=25
            DO 15 J=4, JTOTAL
   15       DY(J) = 0.D0
            JTOTAL=22
            VDT = VD - VT
            IF (NOCOLL)  GO TO 20
C
C     PUT IN COLLISIONAL EFFECTS, IF ANY.  START BY STORING THE RELATIVE
C     VELOCITIES AND THEIR SQUARES.
C
            VDE = VD - VE
            VET = VE - VT
            VTD = -VDT
            VED = -VDE
            VTE = -VET
            VDTSQ = VDT*VDT
            VDESQ = VDE*VDE
            VETSQ = VET*VET
C
            NDMD = ND*MD
            NEME = NE*ME
            NTMT = NT*MT
C
C     FIND COULOMB LOGARITHMS.
C
            LOGLDT = LOGDT0 - .5D0*DLOG(NE/(TE*VDTSQ**2))
            ELOG = .5D0*DLOG(NE/TE**3)
            LOGLDE = LOGDE0 - ELOG
            LOGLTE = LOGTE0 - ELOG
C
```

```
C     CALCULATE THE EFFECTS OF COLLISIONS BETWEEN BEAM AND TARGET IONS.
C     THE LOW-TEMPERATURE LIMIT OF TRUBNIKOV'S FORMULAS IS USED.
C
          NUSDT = CNUSDT*LOGLDT*NT/DABS(VDT**3)
          NUSTD = NUSDT*NDMD/NTMT
          DTDST = CNUTDT*LOGLDT*NT/DABS(VDT)
          NUTDT = DTDST/TD
          DTTSD = DTDST*NDMD/NTMT
          NUTTD = DTTSD/TT
          DWDST = DTDST - KTD*NUSDT*VD*VDT
          DWTSD = DTTSD - KTT*NUSTD*VT*VTD
          IF (U1 .NE. 0.D0)  RNUBYU = RMAJOR*NUSDT/U1
C
C     USE SLOW-BEAM LIMIT TO COMPUTE INTERACTION BETWEEN IONS AND HOT
C     ELECTRONS.
C
          EFACTR = NE/TE**1.5D0
          NUSDE = CNUSDE*LOGLDE*EFACTR
          NUTDE = CNUTDE*LOGLDE*EFACTR
          DTDSE = NUTDE*(TE - TD)
          NUSTE = CNUSTE*LOGLTE*EFACTR
          NUTTE = CNUTTE*LOGLTE*EFACTR
          DTTSE = NUTTE*(TE - TT)
C
C     CONSERVATION OF MOMENTUM GIVES THE REMAINING NUS'S.
C
          NUSED = NUSDE*NDMD/NEME
          NUSET = NUSTE*NTMT/NEME
C
C     USING KNOWN NUS'S AND DT'S, THE CORRESPONDING DW'S ARE FOUND.
C
          DWDSE = DTDSE - KTD*NUSDE*VD*VDE
          DWTSE = DTTSE - KTT*NUSTE*VT*VTE
C
C     CONSERVATION OF ENERGY GIVES THE REMAINING THREE DW'S.
C
          DWESD = -DWDSE*ND/NE
          DWEST = -DWTSE*NT/NE
C
C     FROM THE DERIVED NUS'S AND DW'S, FIND THE REMAINING DT'S.
C
          DTESD = DWESD + KTE*NUSED*VE*VED
          NUTED = DTESD/TE
          DTEST = DWEST + KTE*NUSET*VE*VET
          NUTET = DTEST/TE
C
C     ADD COLLISIONAL CORRECTIONS TO THE DERIVATIVES CALCULATED ABOVE.
C
          DY(JTOTAL) =KPHI*RMAJOR*(NUSED*VED+NUSET*VET)
          DY(7) = -RMAJOR*(NUSDE*VDE + NUSDT*VDT) - KVD*DY(JTOTAL)
          DY(8) = -RMAJOR*(NUSTD*VTD + NUSTE*VTE) - KVT*DY(JTOTAL)
          DY(9) = VGM1*(DTDSE + DTDST)
          DY(10) = VGM1*(DTESD + DTEST)
          DY(11) = VGM1*(DTTSD + DTTSE)
   20     IF (NOLOSS)  GO TO 30
C
C     PUT IN OTHER SOURCES OR SINKS, IF ANY.  START WITH OHMIC LOSSES.
C
          OHMIC=0.D0
          RCONST=KRES*ETA/RLOG
          DO 25 J=1,JMAX1
          RLINER(J)=RCONST/LNGTH(J)
          OHMHT=RLINER(J)*ILINER(J)
          DY(19+J)=-OHMHT
25        OHMIC=OHMIC+OHMHT
C/OUT     DY(5) = DPSI2
```

```
      DY(14) = 0.D0
      DO 26 J=1,JMAX1
26    DY(14) = DY(14) + 1.D7*OHMHT*ILINER(J)
C
C     THEN TREAT LOSSES BY DIFFUSION, CHARGE EXCHANGE, ETC.
C
      DY(10) = DY(10) + TELOSS
      DY(12) = NDLOSS
      DY(13) = NTLOSS
C
C     FINALLY, COMPUTE BREMSSTRAHLUNG AND CYCLOTRON RADIATION LOSSES.
C
      PCYCL = KCYCL*(BETA*BP)**2/(1.D0 - BETA**2)
      PBREM = KBREM*DSQRT(TE)*(ND*ZD*ZD + NT*ZT*ZT)
      PRAD = PBREM + PCYCL
      DTERAD = KT*PRAD
      NURAD = DTERAD/TE
      DY(15) = NETOT*PRAD
      DY(10) = DY(10) - DTERAD*VGM1
30    IF (NOBURN)  GO TO 40
C
C     COMPUTE THERMONUCLEAR BURN.
C
      RATE = SIGMA(1.D3*WD)*DABS(VDT)*ND*NTTOT
      DY(12) = DY(12) - RATE
      DY(13) = DY(13) - RATE
      DY(16) = KNEUTR*RATE
      DY(17) = KBURN*VGM1*RATE
      DY(18) = RATE
40    IF (1 .GT. 0)  RETURN
C
      DO 35 J=4,JTOTAL
35    DY(J)=-DY(J)
      RETURN
C
C     PASS IN DATA NEEDED TO INITIALIZE RUN, SAVING INITIAL VALUES AS Y0.
C     PRECOMPUTE CONSTANTS FOR USE IN SUBSEQUENT CALLS TO DERIV.  CGS
C     UNITS ARE USED THROUGHOUT, EXCEPT THAT TEMPERATURES AND PARTICLE
C     ENERGIES ARE IN KEV AND CIRCUIT QUANTITIES (CURRENTS, FLUXES AND
C     INDUCTANCES) ARE IN MKS.
C
      ENTRY INPUT(TIME,
     1        R10, R20, RW, B20, RH00, OMEGA0, LNGTH0, ETA0, SPHT,
     2        TL00, PCA,
     3        RMAJ0, WD0, TD0, TE0, TT0, BP0, VRATIO, NRATIO, IRATIO,
     4        COLL, LOSS, BURN, FWD,
     5        DTPLOT, DTFILM, DTDUMP, TLAST, TPLOT, TFILM, TDUMP)
      LOGICAL*4 COLL, LOSS, BURN,FWD
      FORWRD=FWD
      RH0 = RH00
      OMEGA = OMEGA0
      ETA = ETA0
      TL0 = TL00
      RMAJOR = RMAJ0
      P=1.D1
      JMAX=3
      JTOTAL=22
      JMAX1=JMAX-1
      DLNGTH=LNGTH0/DFLOAT(JMAX1)
      DO 55 J=1,JMAX1
      LNGTH(J)=DFLOAT(J)*DLNGTH
55    LHLSQ(J)=(0.5D0*LNGTH(J))**2
      NOCOLL = .NOT. COLL
      NOLOSS = .NOT. LOSS
      NOBURN = .NOT. BURN
      DATA E, BOLTZ, C / 4.8032 D-10, 1.6022 D-9, 2.9979 D+10 /
```

```
      DATA MD, ME, MT / 3.3453 D-24, 9.1095 D-28, 5.0179 D-24 /
      DATA ZD, ZT / 1.D0, 2.D0 /
      DATA GAMMA / 1.666666667 D0 /
      DATA DPSI2 / 0.D0 /
      DATA TELOSS, NDLOSS, NTLOSS / 0.D0, 0.D0, 0.D0 /
      DATA 0, RTEST / 1.D-6, 1.D-6 /
      DATA A1, A2, A3, A4, A5 / 2.823 D3, 2.59 D7, 3.98 D-6,
     1     1.297 D0, 6.47 D5 /
      DATA Z / 0.D0 /
      PI = 4.D0*DATAN(1.D0)
      SQRTPI = DSQRT(PI)
      RT2PI = DSQRT(2.D0*PI)
      TWOPI = 2.D0*PI
      FOURPI = 4.D0*PI
      EIGTPI=8.D0*PI
C
C     COMPILE TABLE OF MISCELLANEOUS CONSTANTS.
C
      GM1 = GAMMA - 1.D0
      KBETA = DSQRT(BOLTZ/(GM1*ME*C*C))
      KBREM = 5.35D-24
      KBURN = 18.34D3*BOLTZ*GM1
      KCNVRT = C/1.D1
      KCF = 1.D-7*MD
      KCYCL = 3.98D-16
      KD=0.25D0
      KE = BOLTZ/GM1
      KF=1.D7/(TWOPI*LNGTH0)
      KFLUX = 1.D8/PI
      KID = E*ZD/(TWOPI*KCNVRT)
      KIE=-E/(TWOPI*KCNVRT)
      KIT = E*ZT/(TWOPI*KCNVRT)
      KKIN=PI*RH0*LNGTH0/2.D0
      KMU = FOURPI*1.D-9
      MU = FOURPI*1.D-9
      KNEUTR = 0.D0
      KNKT = 1.D-7*BOLTZ
      KP = 1.D0/(8.D0*PI)
      KPHI = 1. D-8*TWOPI*ME*C/E
      KPROP = MD*C/(ZD*E)
      KR = DSQRT(3.D0*MD*BOLTZ)*C/E
      KRES=1.D2*FOURPI
      KROT=PI*RH0*OMEGA**2*LNGTH0
      KT = GM1/BOLTZ
      KTD = MD*GM1/BOLTZ
      KTE = ME*GM1/BOLTZ
      KTT = MT*GM1/BOLTZ
      KVD = 1.D8*ZD*E/(TWOPI*MD*C)
      KVT = 1.D8*ZT*E/(TWOPI*MT*C)
      KVOL = TWOPI*PI
      KYIELD = KBURN/GM1
C
C     CALCULATE CONSTANTS TO BE USED IN COLLISION RATES.
C
      LOGDE0 = -DLOG(DSQRT(FOURPI/BOLTZ**3)*ZD*E**3)
      LOGDT0 = -DLOG(DSQRT(FOURPI/BOLTZ)*ZD*ZT*E**3*(MD+MT)/(MD*MT))
      LOGTE0 = -DLOG(DSQRT(FOURPI/BOLTZ**3)*ZT*E**3)
C
      CNUSDE = (4.D0*RT2PI/3.D0)*ZD**2*E**4*(1.D0 + MD/ME)*ME**1.5/
     1     (MD**2*BOLTZ**1.5)
      CNUSDT = 4.D0*PI*(ZD*ZT*E**2)**2*(1.D0 + MD/MT)/MD**2
      CNUSTE = (4.D0*RT2PI/3.D0)*ZT**2*E**4*(1.D0 + MT/ME)*ME**1.5/
     1     (MT**2*BOLTZ**1.5)
C
      CNUTDE = (8.D0*RT2PI/3.D0)*(ZD*E*E)**2*DSQRT(ME)/(MD*BOLTZ**
     1     1.5D0)
```

```
      CNUTDT = FOURPI*(ZD*ZT*E*E)**2*GM1/(BOLTZ*MD)
      CNUTTE = (8.D0*RT2PI/3.D0)*(ZT*E*E)**2*DSQRT(ME)/(MT*BOLTZ**
     1         1.5D0)
C
C     DETERMINE LINER CONSTANTS.
C
          R10SQ = R10*R10
          R20SQ = R20*R20
          R0SQ = R20SQ - R10SQ
          RWSQ = RW*RW
          HTCAP=SPHT*PI*R0SQ*LNGTH0*RH0
          PSI20 = B20*(RWSQ - R20SQ)/KFLUX
C
C     DETERMINE INITIAL RING AND PLASMA PARAMETERS.
C
          VD0 = -DSQRT(2.D0*BOLTZ*WD0/MD)
          C1 = PI*RMAJOR/1.D2
          C2 = 5.D0*BP0
          C3 = BOLTZ*(TD0 + NRATIO*TT0 + (ZD + NRATIO*ZT)*TE0)
          C4 = (KID + KIT*NRATIO*VRATIO)*(1.D0 - IRATIO)*VD0/RMAJ0
          IRING = C3/(C1*C4)
          RMIN0 = -IRING/C2
          RMINOR = RMIN0
          VOLUME = KVOL*RMAJOR*RMINOR**2
          VGM1 = VOLUME**GM1
          NDTOT0 = IRING/C4
          ND0 = NDTOT0/VOLUME
          NTTOT0 = NRATIO*NDTOT0
          NT0 = NTTOT0/VOLUME
          VT0 = VRATIO*VD0
          ID0 = KID*NDTOT0*VD0/RMAJ0
          IT0 = KIT*NTTOT0*VT0/RMAJ0
          IE0 = IRING - ID0 - IT0
          RJ0 = R10
C
C     THE INITIAL VALUES OF THE LINER CURRENTS AND NKT ARE NOW FOUND
C     THROUGH A SERIES OF ALGEBRAIC EQUATIONS DESIGNED TO INSURE
C     THAT ZERO FLUX THREADS PERPENDICULAR TO THE LINER AT
C     SPECIFIED POINTS.
C
          JM1=JMAX-2
          DO 41 J=1,JMAX
          DO 41 JJ=1,JMAX
41        ZA(J,JJ)=0.D0
          DO 44 J=1,JM1
          ZA(J,J)=KMU*DLOG((LNGTH(J+1)+LNGTH(J))/(LNGTH(J+1)
     1         -LNGTH(J)))/(TWOPI*LNGTH(J))
          IF(J.EQ.1) GO TO 44
          JP=J-1
          DO 43 JJ=1,JP
          D = (LNGTH(J+1) - LNGTH(JJ)) / 2.D0
          F = LNGTH(JJ)
43        ZA(J,JJ) = (KMU/(TWOPI*LNGTH(JJ))) * DLOG((D+F) / D)
44        CONTINUE
          DO 51 J=1,JMAX1
          ZA(JMAX,J)=DBMLRS(RMIN0,RMAJ0,RJ0,LNGTH(J),LHLSQ(J))
51        ZA(JMAX1,J)=DAMLRS(RMIN0,RMAJ0,RJ0,LNGTH(J),LHLSQ(J))
          ZA(JMAX1,JMAX)=2.D0/(RMIN0*IRING)
          ZA(JMAX,JMAX)=1.D0/(RMAJ0*IRING)
          DO 52 J=1,JM1
          DENOM=(LNGTH(J+1)/2.D0)**2+(RJ0-RMAJ0)**2
          ZR(J)=-(KMU*IRING/FOURPI)*LNGTH(J+1)/DENOM
52        CONTINUE
          ZR(JMAX1)=-0.5D0*IRING*DALR(RMIN0,RMAJ0)
          ZR(JMAX)=-0.5D0*IRING*DBLR(RMIN0,RMAJ0)-KCF*NDTOT0*VD0**2/
     1         (RMAJ0*IRING)
```

```
      JMAX2=JMAX**2
      CALL DGELG(ZR,ZA,JMAX,JMAX2,1,1.D-6,JIER)
      PRINT 42, JIER
42    FORMAT(' ',1X,'IERROR=', I2)
      PRINT 46, (ZR(J),J=1,JMAX)
46    FORMAT(1PSE12.4)
47    CONTINUE
      DO 53 J=1,JMAX1
53    ILINER(J)=ZR(J)
      NKT0=ZR(JMAX)
C
      PHI0=LR(RMIN0,RMAJ0)*IRING
      DO 54 J=1,JMAX1
      D=LNGTH(J)
      F=LHLSQ(J)
      PHI0=PHI0+MLRS(RMIN0,RMAJ0,RJ0,D,F)*ILINER(J)
      PSI1(J)=LL(RJ0,D)*ILINER(J)+MLRS(RMIN0,RMAJ0,RJ0,D,F)*IRING
      DO 62 JJ=1,JMAX1
      IF(J.EQ.JJ) GO TO 62
      PSI1(J) = PSI1(J) + MLL(RJ0,LNGTH(J),LNGTH(JJ))*ILINER(JJ)
62    CONTINUE
      Y(J+19)=PSI1(J)
54    CONTINUE
      NU0 = CNUSDT*2.D1*NT0/(DABS(VD0 - VT0))**3
      U10 = RMAJ0R*NU0/PCA
      IF (FORWRD)  U10 = -U10
C
C     INITIALIZE THE DEPENDENT VARIABLE (Y) ARRAY.
C
      Y(1) = TIME
      Y(2) = R10SQ
      Y(3) = R10*U10
      Y(4) = 0.D0
      Y(5) = PSI20
      Y(6) = 0.D0
      Y(7) = RMAJ0*VD0
      Y(8) = RMAJ0*VT0
      Y(9) = TD0*VGM1
      Y(10) = TE0*VGM1
      Y(11) = TT0*VGM1
      Y(12) = NDT0T0
      Y(13) = NTT0T0
      Y(14) = 0.D0
      Y(15) = 0.D0
      Y(16) = 0.D0
      Y(17) = 0.D0
      Y(18) = 0.D0
      Y(19) = 0.D0
      DO 60 J=1,JMAX1
60    Y(19+J)=PSI1(J)
      Y(JTOTAL)=PHI0
C
C     COPY INITIAL VALUES INTO SAVE ARRAY.
C
      DO 50 J=1,JTOTAL
 50   Y0(J) = Y(J)
C
C     INITIALIZE EXTRAPOLATION PROCEDURE FOR FIRST GUESSES USED IN
C     NEWTON-RAPHSON ROUTINE ON EVEN STEPS OF R-K-G.
C
      DO 61  J = 1, 4
      RMAJ1(J) = RMAJ0
      RMAJ2(J) = RMAJ0
      RMIN1(J) = RMIN0
61    RMIN2(J) = RMIN0
      DTNEW = DT
```

```
      RETURN
C
      ENTRY DSPLAY(SNAME)
      DATA SY, SY0, SDY, SLI, SRING, SPLAS, SNU, SCNU, SDATA /
     1     'Y   ', 'Y0  ', 'DY  ', 'LI  ', 'RING', 'PLAS', 'NU  ',
     2     'CNU ', 'DATA' /
      DATA SBLANK / '    ' /
      DO 100  J = 1, 33
100   SLINE(J) = SBLANK
C
      IF (SNAME .EQ. SY   )  GO TO 110
      IF (SNAME .EQ. SY0  )  GO TO 120
      IF (SNAME .EQ. SDY  )  GO TO 130
      IF (SNAME .EQ. SLI  )  GO TO 140
      IF (SNAME .EQ. SRING)  GO TO 150
      IF (SNAME .EQ. SPLAS)  GO TO 160
      IF (SNAME .EQ. SNU  )  GO TO 170
      IF (SNAME .EQ. SCNU )  GO TO 180
      IF (SNAME .EQ. SDATA)  GO TO 190
      PRINT 101, SNAME
101   FORMAT('0', 'DSPLAY CALLED WITH INVALID ARGUMENT ', A4 //)
      RETURN
C
C     DEPENDENT VARIABLES.
C
110   PRINT 111
111   FORMAT('-  Y(1)    Y(2)    Y(3)    Y(5)    Y(6)    Y(7)    ',
     1     'Y(9)    Y(10)   Y(11)   Y(12)   Y(13)   Y(14)   Y(15)',
     2     '   Y(16)   Y(17)   Y(18)')
      CALL SCNVRS(SLINE, Y(1), Y(2), Y(3), Y(5), Y(6), Y(7), Y(9),
     1     Y(10), Y(11), Y(12), Y(13), Y(14), Y(15), Y(16), Y(17),
     2     Y(18))
      PRINT 199, SLINE
      RETURN
C
C     INITIAL VALUES OF DEPENDENT VARIABLES.
C
120   PRINT 121
121   FORMAT('-  Y0(1)   Y0(2)   Y0(3)   Y0(5)   Y0(6)   Y0(7)   ',
     1     'Y0(9)   Y0(10)  Y0(11)  Y0(12)  Y0(13)  Y0(14)  Y0(15)',
     2     '  Y0(16)  Y0(17)  Y0(18)')
      CALL SCNVRS(SLINE, Y0(1), Y0(2), Y0(3), Y0(5), Y0(6), Y0(7),
     1     Y0(9), Y0(10), Y0(11), Y0(12), Y0(13), Y0(14), Y0(15),
     2     Y0(16), Y0(17), Y0(18))
      PRINT 199, SLINE
      RETURN
C
C     DERIVATIVES OF DEPENDENT VARIABLES.
C
130   PRINT 131
131   FORMAT('-  DY(1)   DY(2)   DY(3)   DY(5)   DY(6)   DY(7)   ',
     1     'DY(9)   DY(10)  DY(11)  DY(12)  DY(13)  DY(14)  DY(15)',
     2     '  DY(16)  DY(17)  DY(18)')
      CALL SCNVRS(SLINE, DY(1), DY(2), DY(3), DY(5), DY(6), DY(7),
     1     DY(9), DY(10), DY(11), DY(12), DY(13), DY(14), DY(15),
     2     DY(16), DY(17), DY(18))
      PRINT 199, SLINE
      RETURN
C
C     LINER PARAMETERS AND ENERGETICS.
C
140   PRINT 141
141   FORMAT('-   R1      R2      U1      U2      G1      G2    ',
     1     '  B1      B2      ETA      PSI2   RSKIN  PSI1(1) PSI1(2)',
     2     ' PSI1(3) PSI1(4) PSI1(5)')
```

```
      1        PSI2, RJ, PSI1(1), PSI1(2), PSI1(3), PSI1(4), PSI1(5))
               PRINT 199, SLINE
               PRINT 142
  142          FORMAT('=  ETOT     EKIN     EROT     EPOT     EMAG     EMAG2   ',
      1        'ERING   EBEAM   EDDIR   EDTH    EPLAS   EETH    ETTH   ',
      1        ' ETDIR   ENET      Q')
               CALL SCNVRS(SLINE, ETOT, EKIN, EROT, EPOT, EMAG, EMAG2,
      1        ERING, EBEAM, EDDIR, EDTH, EPLAS, EETH, ETTH, ETDIR,
      1        ENET, Q)
               PRINT 199, SLINE
               PRINT 143
  143          FORMAT('= EMAG(1) EMAG(2) EMAG(3) EMAG(4) EMAG(5)   IL1     ',
      1       'IL2      IL3      IL4      IL5      RL1      RL2      RL3   ',
      2        ' RL4      RL5      TL')
               CALL SCNVRS(SLINE, EMAG1(1), EMAG1(2), EMAG1(3), EMAG1(4),
      1        EMAG1(5), ILINER(1), ILINER(2), Z,Z,Z,
      2         RLINER(1), RLINER(2), RLINER(3), RLINER(4),
      3        RLINER(5), TL)
               PRINT 199, SLINE
               RETURN
C
C      PARAMETERS OF ION AND IMAGE RINGS.
C
  150          PRINT 151
  151          FORMAT('=  RMAJOR  RMINOR   IRING    ID      LRING    MLR1    ',
      1        ' PHI      PD       VD       WD      NDTOT    ND       TD     ',
      1        'VOLUME   ITER     RATE')
               CALL SCNVRS(SLINE, RMAJOR, RMINOR, IRING, ID, LRING, MLR1S,
      1        PHI, PD, VD, WD, NDTOT, ND, TD, VOLUME, ITER, RATE)
               PRINT 199, SLINE
               RETURN
C
C      TARGET PLASMA AND RADIATION PARAMETERS.
C
  160          PRINT 161
  161          FORMAT('=  NETOT   NTTOT  VOLUME    NE       NT       WT      ',
      1        'VE       VT       PTOT     TE       TT       PE       PT    ',
      2        '    IE       IT      YIELD')
               CALL SCNVRS(SLINE, NETOT, NTTOT, VOLUME, NE, NT, WT, VE, VT,
      1        PTOT, TE, TT, PE, PT, IE, IT, YIELD)
               PRINT 199, SLINE
               PRINT 162
  162          FORMAT('=  BETA      BP      PCYCL    PBREM    PRAD     NURAD   ',
      1        ' ERAD    DTERAD    PPOL    RNUBYU   NCOUNT   BETAPL   EOHMIC ',
      2        '  KAPPA   PVGPRD   BURNUP')
               CALL SCNVRS(SLINE, BETA, BP, PCYCL, PBREM, PRAD, NURAD, ERAD,
      1        DTERAD, PPOL, RNUBYU, NCOUNT, BETAPL, EOHMIC, KAPPA,
      2        PVGPRD, BURNUP)
               PRINT 199, SLINE
               RETURN
C
C      TRANSPORT RATES.
C
  170          PRINT 171
  171          FORMAT('=  NUSDE    NUSDT    NUSTE    NUSED    NUSTD    NUSET   ',
      1        ' VDT      VDE      VET      ELOG     DWD/E    DWD/T    DWT/E ',
      2        '  DWE/D    DWT/D    DWE/T')
               CALL SCNVRS(SLINE, NUSDE, NUSDT, NUSTE, NUSED, NUSTD, NUSET,
      1        VDT, VDE, VET, ELOG, DWDSE, DWDST, DWTSE, DWESD, DWTSD,
      2        DWEST)
               PRINT 199, SLINE
               PRINT 172
  172          FORMAT('=  NUTDE    NUTDT    NUTET    NUTED    NUTTD    NUTTE   ',
      1        'DTD/E    DTD/T    DTE/T    DTE/D    DTT/D    DTT/E  LOGLDE',
      2        '  LOGLDT  LOGLTE')
C     REPORT CALL SCNVRS(SLINE, NUTDE, NUTDT, NUTET, NUTED, NUTTD, NUTTE,
```

```
     1        DTDSE, DTDST, DTESY, DTESD, DTTSC, CTTSE, LOGLDE, LOGLDT,
     2        LOGLTE, Z)
              PRINT 199, SLINE
C
C     INDUCTANCES.
C
              PRINT 173
173           FORMAT('=  LL1     LL2     LL3     LL4     LL5   THIS SPACE',
     1        ' FOR RENT ')
              CALL SCNVRS(SLINE, LL1, LL2, LL3, LL4, LL5, Z, Z , Z, Z, Z,
     1        Z, Z, Z, Z, Z, Z)
              PRINT 199, SLINE
              PRINT 175
175           FORMAT('=  LL5     ML12    ML13    ML14    ML15    ML23    ',
     1        'ML24    ML25    ML34    ML35    ML45    MLRS1   MLRS2 ',
     2        '  MLRS3   MLRS4   MLRS5 ')
              CALL SCNVRS(SLINE, LL5, ML12, ML13, ML14, ML15, ML23, ML24,
     1        ML25, ML34, ML35, ML45, MLRS1, MLRS2, MLRS3, MLRS4, MLRS5)
              PRINT 199, SLINE
              RETURN
C
C     CONSTANTS USED IN EVALUATING TRANSPORT AND RADIATION RATES.
C
 180          PRINT 181
 181          FORMAT('=  LOGDE0  LOGDT0  LOGTE0    KTD     KTE     KTT   ',
     1        'CNUSDE  CNUSDT  CNUSTE  CNUTDE  CNUTDT  CNUTTE   KBETA ',
     2        '  KBREM   KCYCL    KT')
              CALL SCNVRS(SLINE, LOGDE0, LOGDT0, LOGTE0, KTD, KTE, KTT,
     1        CNUSDE, CNUSDT, CNUSTE, CNUTDE,CNUTDT, CNUTTE, KBETA,
     2        KBREM, KCYCL, KT)
              PRINT 199, SLINE
              RETURN
C
C     PHYSICAL CONSTANTS AND STORED COMBINATIONS THEREOF.
C
 190          PRINT 191
 191          FORMAT('=     E      BOLTZ     C       MD      ME      MT   ',
     1        '    ZD      ZT      RW    LENGTH  TELOSS  NDLOSS  NTLOSS',
     2        '   OPSI2   OMEGA   GAMMA')
              CALL SCNVRS(SLINE, E, BOLTZ, C, MD, ME, MT, ZD, ZT, RW,
     1        LNGTH0, TELOSS, NDLOSS, NTLOSS, OPSI2, OMEGA, GAMMA)
              PRINT 199, SLINE
              PRINT 192
 192          FORMAT('=  KBURN  KCNVRT    KCF     KD      KE      KF     ',
     1        'KFLUX    KID     KIE     KIT    KKIN     KMU   KNEUTR  ',
     2        ' KNKT     KP     KPROP')
              CALL SCNVRS(SLINE, KBURN, KCNVRT, KCF, KD, KE, KF, KFLUX,
     1        KID, KIE, KIT, KKIN, KMU, KNEUTR, KNKT, KP, KPROP)
              PRINT 199, SLINE
              PRINT 193
 193          FORMAT('=  KPHI     KR      KRES    KROT    KVD     KVT   ',
     1        ' KVOL     KVD     KVT   KYIELD    OR    RTEST    SPHT  ',
     2        '  HTCAP')
              CALL SCNVRS(SLINE, KPHI, KR, KRES, KROT, KVD, KVT, KVOL, KVD,
     1        KVT, KYIELD, O, RTEST, SPHT, HTCAP, Z, Z)
              PRINT 199, SLINE
              PRINT 194
 194          FORMAT('=   DT     DTPLOT  DTFILM  DTDUMP   TLAST     T     ',
     1        'TPLOT   TFILM   TDUMP  IRATIO  VRATIO  NRATIO')
              CALL SCNVRS(SLINE, DT, DTPLOT, DTFILM, DTDUMP, TLAST, TIME,
     1        TPLOT, TFILM, TDUMP, IRATIO, VRATIO, NRATIO, Z, Z, Z, Z)
              PRINT 199, SLINE
              RETURN
C
 199          FORMAT(' ', 33A4)
```

```
C
      ENTRY OUTPUT
          RETURN
          E N D
C
          REAL FUNCTION FA*8(A,B,C,NKT)
          IMPLICIT REAL*8(A-I,K-Z), INTEGER*4(J)
          DIMENSION YA(3,3)
          COMMON / INDEX / JMAX, JMAX1
          COMMON / PBLOCK / P
          COMMON/ RADII/ RMINOR,RMAJOR,RJ
          COMMON/ LENGTH/  LNGTH(5), LHLSQ(5)
          COMMON/ ARRAY/ Y(25), DY(25), Y0(25)
          COMMON / INCO / MU, KMU
          COMMON/ FLUX/ PHI,PSI1(5)
          COMMON / CURREN / R(3)
          LR(A,B) = KMU*B*(DLOG(8.D0*B/A) - 2.D0 + KD)
          DALR(A,B) = -KMU*B/A
          DBLR(A,B) = KMU*(DLOG(8.D0*B/A) - 1.D0 + KD)
          LL(C,D)=MU*C*(DLOG(16.D0*C/D) - 0.5D0)
          DCLL(C,D)=MU*(DLOG(16.D0*C/D) + 0.5D0)
          LN(D,F)=0.5D0*(D/F)*DLOG(D)
          FAC(D,F)=(((F-D)**2)/(2.D0*D*F))*DLOG(DABS(F-D))
          MLL(C,D,F)=MU*C*(DLOG(16.D0*C)-LN(D,F)-LN(F,D)+FAC(D,F)-0.5D0)
          DCMLL(C,D,F)=MU*(DLOG(16.D0*C)-LN(D,F)-LN(F,D)+FAC(D,F)+0.5D0)
          MLR(B,C,F)=MU*DSQRT(B*C)*(.5D0*DLOG(6.4D1*B*C/((B-C)**2 +
     1         F)) - 1.D0 - ((B-C)/DSQRT(F))*DATAN(DSQRT(F)/(B-C)))
          DBMLR(B,C,F)=.5D0*MU*DSQRT(C/B)*(.5D0*DLOG(6.4D1*B*C/((B-C)**2
     1         +F))+((C-3.D0*B)/DSQRT(F))*DATAN(DSQRT(F)/(B-C)))
          DCMLR(B,C,F)=.5D0*MU*DSQRT(B/C)*(.5D0*DLOG(6.4D1*B*C/((B-C)**2
     1         +F))+((3.D0*C-B)/DSQRT(F))*DATAN(DSQRT(F)/(B-C)))
          MLRS(A,B,C,D,F)=MLR(B,C,F)+(DSQRT(LR(A,B)*LL(C,D))-MLR(B,C,F))
     1         /(1.D0+((C-B)/A)**P)
          DAMLRS(A,B,C,D,F)=(.5D0*DALR(A,B)*DSQRT(LL(C,D)/LR(A,B))+(P/A)
     1         *((C-B)/A)**P*(DSQRT(LR(A,B)*LL(C,D))-MLR(B,C,F))/(1.D0+
     2         ((C-B)/A)**P))/(1.D0 + ((C-B)/A)**P)
          DBMLRS(A,B,C,D,F)=DBMLR(B,C,F)+(.5D0*DBLR(A,B)*DSQRT(LL(C,D)/
     1         LR(A,B)) + (P/(C-B))*((C-B)/A)**P*(DSQRT(LR(A,B)*LL(C,D))-
     2       MLR(B,C,F))/(1.D0 + ((C-B)/A)**P))/(1.D0 + ((C-B)/A)**P)
          DCMLRS(A,B,C,D,F)=DCMLR(B,C,F)+(.5D0*DCLL(C,D)*DSQRT(LR(A,B)/
     1         LL(C,D))-(P/(C-B))*(((C-B)/A)**P*(DSQRT(LR(A,B  )*LL(C,D))-
     2       MLR(B,C,F))/(1.D0 + ((C-B)/A)**P))/(1.D0 + ((C-B)/A)**P)
C      A SERIES OF ALGEBRAIC EQUATIONS IS SOLVED TO FIND THE CURRENTS
C      IN THE LINER AND RING.
          KD = .25D0
          MINR=A
          MAJR=B
          LIR=C
          LIR2=LIR
          JMAXM=JMAX-1
          DO 1 J=1,JMAXM
1         R(J)=Y(19+J)
          R(JMAX)=Y(19+JMAX)
          YA(1,1)= LL(LIR,LNGTH(1))
          DO 2 J1=2,JMAXM
          A1=LNGTH(J1)
          YA(J1,J1)=LL(LIR,A1)
          JIMI=J1-1
          DO 2 J2=1,JIMI
          F=LNGTH(J2)
          YA(J1,J2)=MLL(LIR,A1,F)
          YA(J2,J1)=YA(J1,J2)
2         CONTINUE
          DO 4 J=1,JMAXM
          A1=LNGTH(J)
          D=LHLSQ(J)
```

```
184067      YA(JMAX,J)=MLRS(MINR,MAJR,LIR,A1,D)
            YA(J,JMAX)=YA(JMAX,J)
           YA(JMAX,JMAX)=LR(MINR,MAJR)
            JMAX2=JMAX**2
            CALL DGELG (R, YA, JMAX, JMAX2, 1, 1.D-6, JIER)
            FA            =0.5D0*R(JMAX)**2*DALR(A,B)+2.D0*NKT/A
            DO 20 J=1,JMAX1
            D=LNGTH(J)
            F=LHLSQ(J)
20          FA            =FA            +R(JMAX)*R(J)*DAMLRS(A,B,C,D,F)
            RETURN
            END
            REAL FUNCTION FB*8(A,B,C,NKT)
            IMPLICIT REAL*8(A-I,K-Z), INTEGER*4(J)
            DIMENSION YA(3,3)
            COMMON / INCO / MU, KMU
            COMMON/ COEFF/ KCF,NDTOT, RVD
            COMMON / PBLOCK / P
            COMMON / CURREN / R(3)
            COMMON/ LENGTH/  LNGTH(5), LHLSQ(5)
            COMMON / INDEX / JMAX, JMAX1
            COMMON/ ARRAY/ Y(25), DY(25), Y0(25)
            COMMON/ RADII/ RMINOR,RMAJOR,RJ
            COMMON/ FLUX/ PHI,PSI1(5)
            LR(A,B) = KMU*B*(DLOG(8.D0*B/A) - 2.D0 + KD)
            DALR(A,B) = -KMU*B/A
            DBLR(A,B) = KMU*(DLOG(8.D0*B/A) - 1.D0 + KD)
            LL(C,D)=MU*C*(DLOG(16.D0*C/D) - 0.5D0)
            DCLL(C,D)=MU*(DLOG(16.D0*C/D) + 0.5D0)
            LN(D,F)=0.5D0*(D/F)*DLOG(D)
            FAC(D,F)=(((F-D)**2)/(2.D0*D*F))*DLOG(DABS(F-D))
            MLL(C,D,F)=MU*C*(DLOG(16.D0*C)-LN(D,F)-LN(F,D)+FAC(D,F)-0.5D0)
            DCMLL(C,D,F)=MU*(DLOG(16.D0*C)-LN(D,F)-LN(F,D)+FAC(D,F)+0.5D0)
            MLR(B,C,F)=MU*DSQRT(B*C)*(.5D0*DLOG(6.4D1*B*C/((B-C)**2 +
     1          F)) - 1.D0 - ((B-C)/DSQRT(F))*DATAN(DSQRT(F)/(B-C)))
            DBMLR(B,C,F)=.5D0*MU*DSQRT(C/B)*(.5D0*DLOG(6.4D1*B*C/((B-C)**2
     1          +F))+((C-3.D0*B)/DSQRT(F))*DATAN(DSQRT(F)/(B-C)))
            DCMLR(B,C,F)=.5D0*MU*DSQRT(B/C)*(.5D0*DLOG(6.4D1*B*C/((B-C)**2
     1          +F))+((3.D0*C-B)/DSQRT(F))*DATAN(DSQRT(F)/(B-C)))
            MLRS(A,B,C,D,F)=MLR(B,C,F)+(DSQRT(LR(A,B)*LL(C,D))-MLR(B,C,F))
     1          /(1.D0+((C-B)/A)**P)
            DAMLRS(A,B,C,D,F)=(.5D0*DALR(A,B)*DSQRT(LL(C,D)/LR(A,B))+(P/A)
     1          *((C-B)/A)**P*(DSQRT(LR(A,B)*LL(C,D))-MLR(B,C,F))/(1.D0+
     2          ((C-B)/A)**P))/(1.D0 + ((C-B)/A)**P)
            DBMLRS(A,B,C,D,F)=DBMLR(B,C,F)+(.5D0*DBLR(A,B)*DSQRT(LL(C,D)/
     1          LR(A,B)) + (P/(C-B))*((C-B)/A)**P*(DSQRT(LR(A,B)*LL(C,D))-
     2        MLR(B,C,F))/(1.D0 + ((C-B)/A)**P))/(1.D0 + ((C-B)/A)**P)
            DCMLRS(A,B,C,D,F)=DCMLR(B,C,F)+(.5D0*DCLL(C,D)*DSQRT(LR(A,B)/
     1          LL(C,D))-(P/(C-B))*((C-B)/A)**P*(DSQRT(LR(A,B  )*LL(C,D))-
     2        MLR(B,C,F))/(1.D0 + ((C-B)/A)**P))/(1.D0 + ((C-B)/A)**P)
C       A SERIES OF ALGEBRAIC EQUATIONS IS SOLVED TO FIND THE CURRENTS
C       IN THE LINER AND RING.
            KD = .25D0
            MINR=A
            MAJR=B
            LIR=C
            LIR2=LIR
            JMAXM=JMAX-1
            DO 1 J=1,JMAXM
1           R(J)=Y(19+J)
            R(JMAX)=Y(19+JMAX)
            YA(1,1)= LL(LIR,LNGTH(1))
            DO 2 J1=2,JMAXM
            A1=LNGTH(J1)
           YA(J1,J1)=LL(LIR,A1)
            JIMI=J1-1
```

```
      DO 2 J2=1,JIMI
      F=LNGTH(J2)
     YA(J1,J2)=MLL(LIR,A1,F)
      YA(J2,J1)=YA(J1,J2)
2     CONTINUE
      DO 4 J=1,JMAXM
      A1=LNGTH(J)
      D=LHLSQ(J)
     YA(JMAX,J)=MLRS(MINR,MAJR,LIR,A1,D)
4     YA(J,JMAX)=YA(JMAX,J)
     YA(JMAX,JMAX)=LR(MINR,MAJR)
      JMAX2=JMAX**2
      CALL DGELG (R, YA, JMAX, JMAX2, 1, 1.D-6, JIER)
      FB=0.5D0*R(JMAX)**2*DBLR(A,B)+NKT/B+KCF*NDTOT*RVD**2/B**3
      DO 20 J=1,JMAXI
      D=LNGTH(J)
      F=LHLSQ(J)
20    FB          =FB          +R(JMAX)*R(J)*DBMLRS(A,B,C,D,F)
      RETURN
      END
```

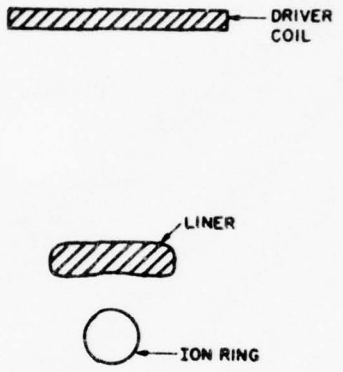

Fig. 1 – Schematic of a fixed driver coil and moving liner and ion beam plasma ring, all having finite length and roughly satisfying the large-aspect ratio approximation.

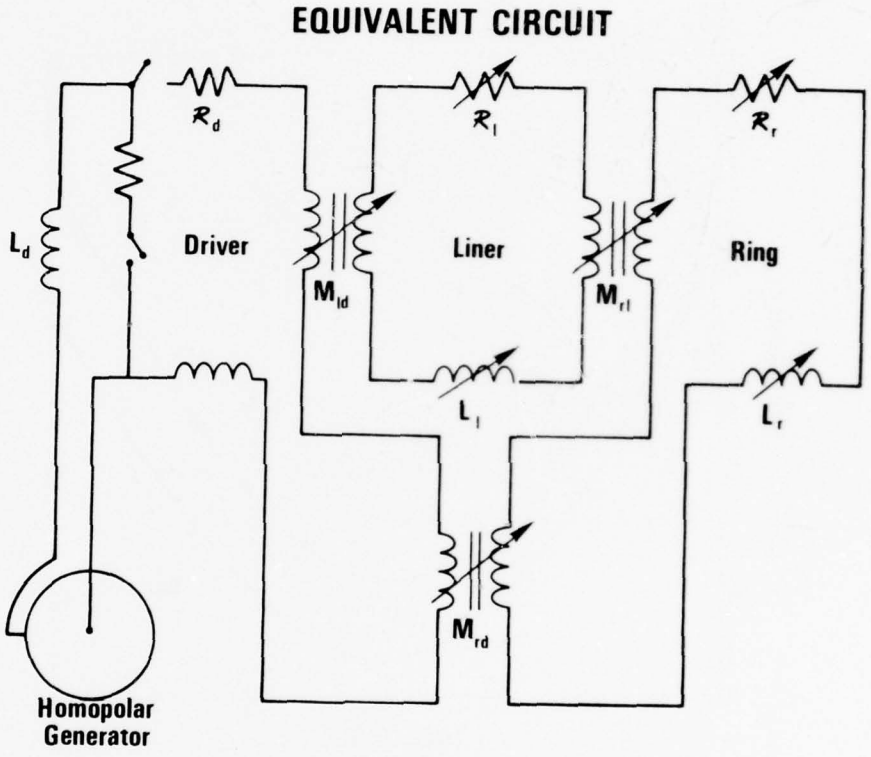

Fig. 2 – Electrical circuit equivalent to Fig. 1. A homopolar generator is used to energize the driving coil.

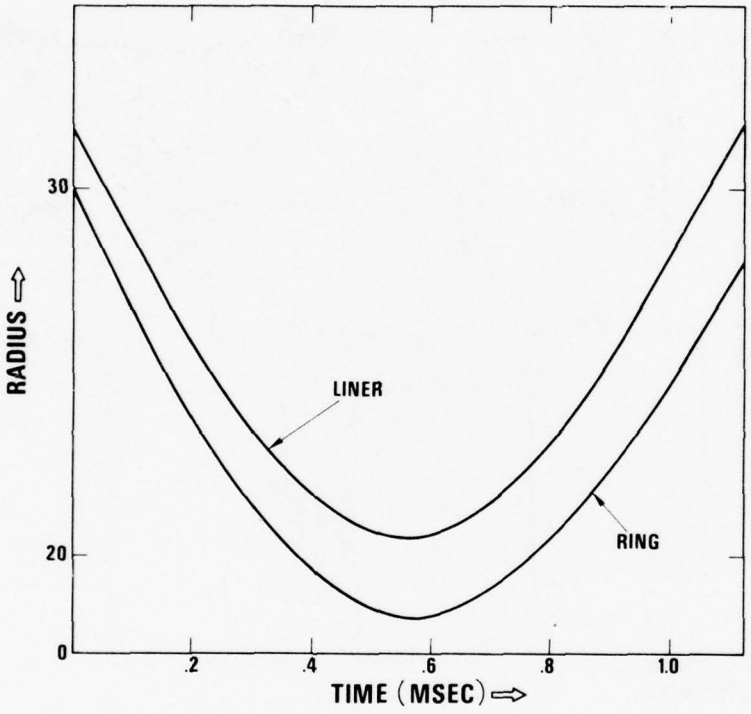

Fig. 3 – Ring and liner radii vs t for the given initial conditions.

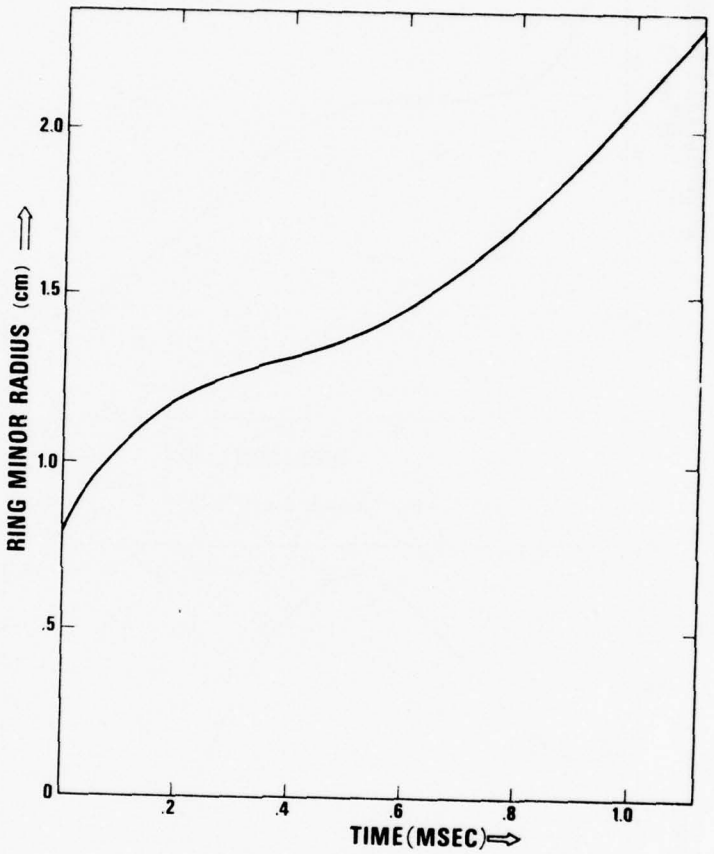

Fig. 4 – Ring minor radius vs. t.

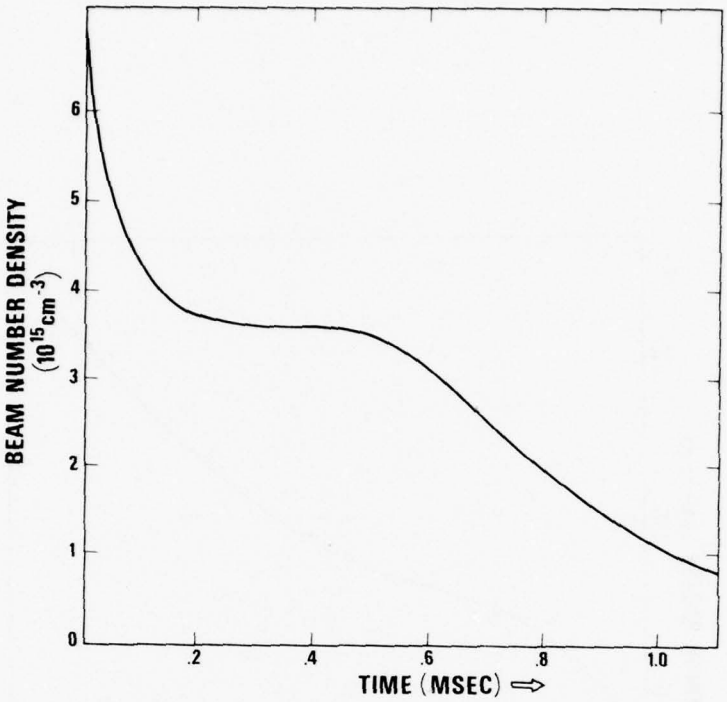

Fig. 5 – Beam number density vs. t.

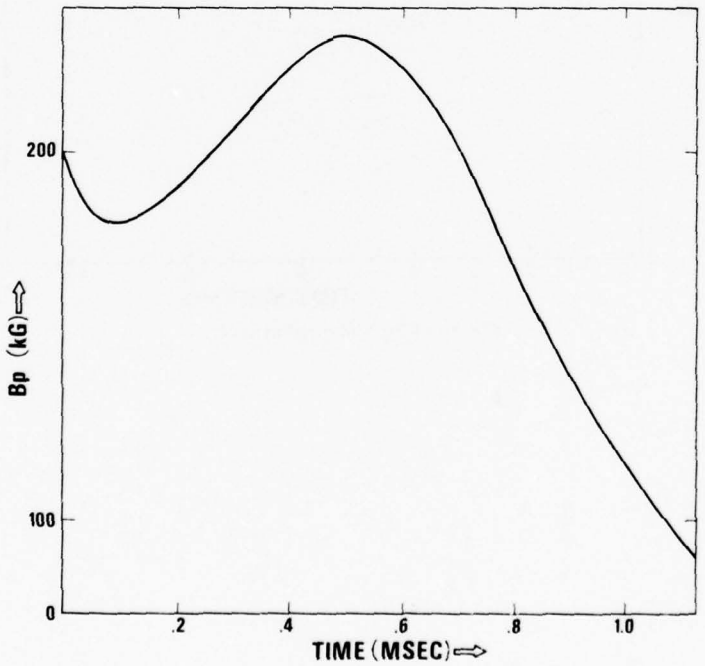

Fig. 6 – Poloidal magnetic field vs t.

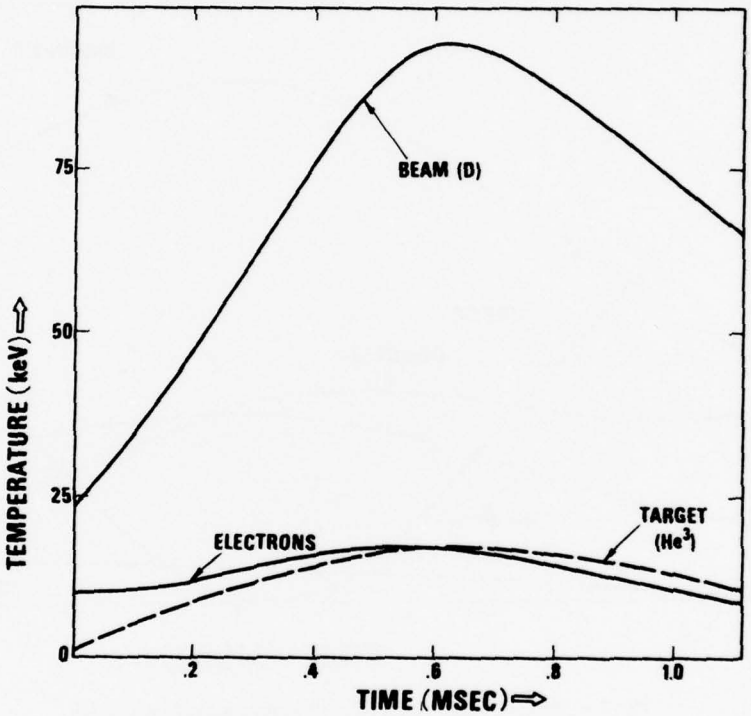

Fig. 8 – Beam, target ion and electron temperatures vs. *t*.

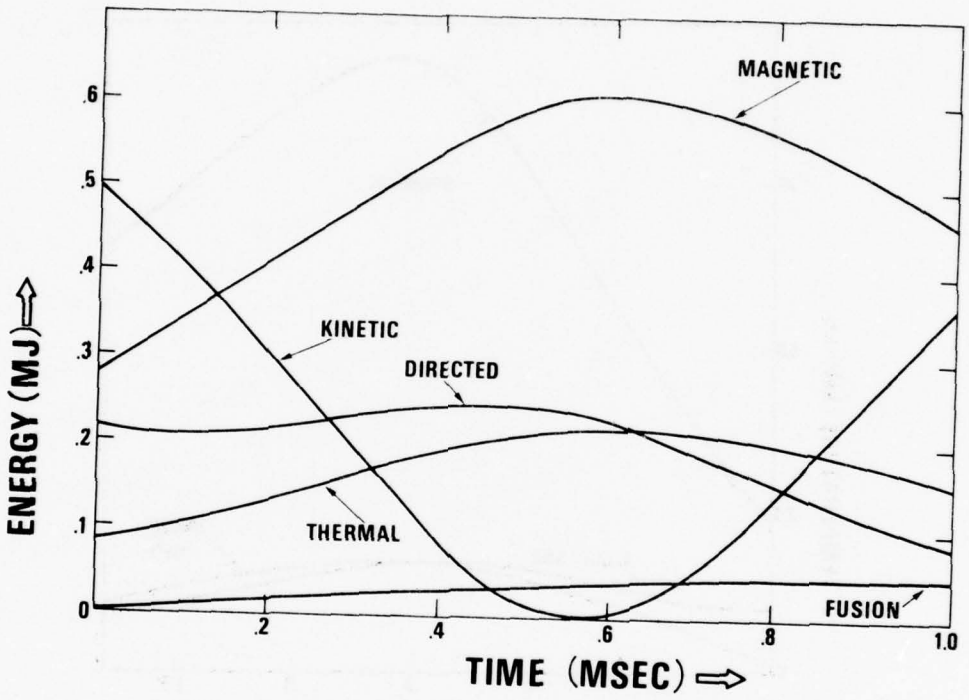

Fig. 7 – Magnetic energy [from Eq. (9)], liner kinetic energy, ion streaming energy, and total particle thermal energy vs. t.

DISTRIBUTION LIST

Defense Documentation Center
Cameron Station
Alexandria, VA 22314 12 copies

Technical Library
David W. Taylor Naval Ship Research
and Development Center
Annapolis Laboratory
Annapolis, MD 21402

Professor Bruce Johnson
Engineering Department
Naval Academy
Annapolis MD 21402

Library
Naval Academy
Annapolis, MD 21402

Professor T. Francis Ogilvie
Department of Naval Architecture
and Marine Engineering
University of Michigan
Ann Arbor, MI 48105

Professor C. S. Yih
Department of Engineering Mechanics
University of Michigan
Ann Arbor, MI 48105

Dr. Code Pan
Shaker Research Corporation
Northway 10 Executive Park
Ballston Lake, NY 12019

NASA Scientific and Technical Information
Facility
P. O. Box 8757
Baltimore/Washington International Airport
Maryland 21240

A. H. Makomasi
Mechanical Engineering Division
National Research Council of Canada
Ottawa, Canada
KIA ÒR6

S. A. Thorpe
National Institute of Oceanography
Wormley, Godalming, Surrey
England

P. C. Patnaik
Science Applications, Inc.
1205 Prospect Street
La Jolla, CA 92037

F. S. Sherman
Department of Mechanical Engineering
University of California
Berkeley, CA 94720

Fred Fajen
Mission Research Corporation
P. O. Drawer 719
Santa Barbara, Calif. 93102

Dr. Harvey R. Chaplin
Code 16
Naval Ship Research and Development Center
Bethesda, MD 20034

Mr. Robert Moore
Deputy Director, Tactical
Technology Office
Defense Advanced Research Projects Agency
1400 Wilson Boulevard
Arlington, VA 22209

A. B. Langdon
Lawrence Livermore Laboratory
Livermore, California 94550

W. P. Crowley
Lawrence Livermore Laboratory
Livermore, Calif. 94550

Dr. Robert Voight
ICASE
Mail Stop 132C
NASA Langley Research Center
Hampton, VA 23665

Dr. James Ortega
ICASE
Mail Stop 132C
NASA Langley Research Center
Hampton, VA 23665

Dr. William Buzbee
P. O. Box 1663
Los Alamos Scientific Laboratory
Los Alamos, NM 87344

Dr. James Welch
Princeton Geophysical Laboratory
Princeton, NJ 08540

Dr. Francis J. Balint
Naval Oceanic and Atmospheric Administration
Bldg. 5 - AD3
6010 Executive Blvd.
Rockville, MD 20852

Mr. John L. Hess
Douglas Aircraft Company
3855 Lakewood Boulevard
Long Beach, CA 90801

Dr. H. K. Cheng
Department of Aerospace Engineering
University of Southern California
University Park
Los Angeles, CA 90007

Dr. J. Trulio
Applied Theory, Inc.
1010 Westwood Blvd.
Los Angeles, CA 90024

Dr. T. D. Taylor
The Aerospace Corporation
Post Office Box 95085
Los Angeles, CA 90045

Dr. J. R. Spreiter
Nielsen Engineering and Research, Inc.
850 Maude Avenue
Mountain View, CA 94040

Professor S. I. Cheng
Gas Dynamics Laboratory
Forrestal Campus
Princeton University
Princeton, NJ 08540

Dr. H. Yoshihara
Mail Zone 630-00
General Dynamics-CONVAIR
P. O. Box 1128
San Diego, CA 92112

Dr. R. J. Hakkinen
Department 222
McDonnell Douglas Corporation
P. O. Box 516
St. Louis, MO 63166

Mr. R. Siewert (AIR 320D)
Naval Air Systems Command
Washington, D. C. 20361

Chief of Research and Development
Office of Chief of Staff
Department of the Army
Washington, DC 20310

Dr. G. Kulin
Fluid Mechanics Section
National Bureau of Standards
Washington, DC 20234

National Science Foundation
Engineering Division
1800 G Street, NW
Washington, DC 20550

Science and Technology Division
Library of Congress
Washington, DC 20540

Defense Research and Development Attache
Australian Embassy
1601 Massachusetts Avenue, NW
Washington, DC 20036

Dr. A. S. Iberall, President
General Technical Services, Inc.
451 Penn Street
Yeadon, PA 19050

Dr. Ricardo A. Bastianon
Instituto de Tecnologia Naval
E.E.V.V. 25 - Capital Federal
Buenos Aires, Argentina

Professor James C. Wu
School of Aerospace Engineering
Georgia Institute of Technology
Atlanta, GA 30332

Professor A. J. Chorin
Department of Mathematics
University of California
Berkeley, CA 94720

Dr. S. A. Berger
Department of Mechanical Engineering
University of California
Berkeley, CA 94720

Dr. G. R. Inger
Department of Aerospace Engineering
Virginia Polytechnic Institute
Blacksburg, VA 24061

Professor A. H. Nayfeh
Department of Engineering Mechanics
Virginia Polytechnic Institute
Blacksburg, VA 24061

Dr. John D. Anderson, Jr.
Chairman, Department of Aerospace
Engineering
College of Engineering
University of Maryland
College Park, MD 20742

Professor R. T. Davis
Department of Aerospace Engineering
and Applied Mechanics
University of Cincinnati
Cincinnati, OH 45221

Professor O. Burggraf
Department of Aeronautical and
Astronautical Engineering
Ohio State University
Columbus, OH 43220

Dr. W. R. Briley
United Aircraft Corporation Research
Laboratory
East Hartford, CT 06108

Dr. S. Nadir
Northrop Corporation
Aircraft Division
3901 West Broadway
Hawthorne, CA 90250

Technical Library
Naval Ordnance Station
Indian Head, MD 20640

Professor S. F. Shen
Graduate School of Aerospace
Engineering
Cornell University
Ithaca, NY 14850

Strategic Systems Projects Office
Department of the Navy
Washington, DC 20376

Mr. Norman Nilsen (SP 2022)
Strategic Systems Projects Office
Department of the Navy
Washington, DC 20376

Oceanographer of the Navy
200 Stovall Street
Alexandria, VA 22332

Commander
Naval Oceanographic Office
Washington, DC 20373

Dr. A. L. Slafkosky
Scientific Advisor
Commandant of the Marine Corps (Code AX)
Washington, DC 20380

Librarian Station 5-2
Coast Guard Headquarters
NASSIF Building
400 Seventh Street, SW
Washington, DC 20591

Office of Research and Development
Maritime Administration
411 G Street, NW
Washington, DC 20235

Division of Ship Design
Maritime Administration
441 G Street, NW
Washington, DC 20235

Air Force Office of Scientific
Research/NA
Building 410
Bolling AFB
Washington, DC 20332

AFDRD-AS/M
U. S. Air Force
The Pentagon
Washington, DC 20330

Mr. G. H. Gleissner (Code 18)
David W. Taylor Naval Ship Research
and Development Center
Bethesda, MD 20084

Dr. P. C. Pien (Code 1520)
David W. Taylor Naval Ship Research
and Development Center
Bethesda, MD 20084

Mr. Paul S. Granville (Code 1541)
David W. Taylor Naval Ship Research
and Development Center
Bethesda, MD 20084

Mr. J. H. McCarthy, Jr. (Code 1552)
David W. Taylor Naval Ship Research
and Development Center
Bethesda, MD 20084

Dr. Nils Salvesen (Code 1552)
David W. Taylor Naval Ship Research
and Development Center
Bethesda, MD 20084

Mrs. Joanna Schot (Code 1843)
David W. Taylor Naval Ship Research
and Development Center
Bethesda, MD 20084

Library (Code 5641)
David W. Taylor Naval Ship Research
and Development Center
Bethesda, MD 20084

Code 03
Naval Air Systems Command
Washington, DC 20361

Code 03B
Naval Air Systems Command
Washington, DC 20361

Code 310
Naval Air Systems Command
Washington, DC 20361

Code 5301
Naval Air Systems Command
Washington, DC 20361

Code 6034
Naval Ship Engineering Center
Center Building
Prince Georges Center
Hyattsville, MD 20782

Code 6101E
Naval Ship Engineering Center
Center Building
Prince Georges Center
Hyattsville, MD 20782

Code 6110
Naval Ship Engineering Center
Center Building
Prince Georges Center
Hyattsville, MD 20782

Code 6114
Naval Ship Engineering Center
Center Building
Prince Georges Center
Hyattsville, MD 20782

Code 6136
Naval Ship Engineering Center
Center Building
Prince Georges Center
Hyattsville MD 20782

Code 6140
Naval Ship Enginnering Center
Center Building
Prince Georges Center
Hyattsville, MD 20782

Dr. A. Powell (Code 01)
David W. Taylor Naval Ship
Research and Development Center
Bethesda, MD 20084

Dr W. E. Cummins (Code 15)
David W. Taylor Naval Ship Research
and Development Center
Bethesda, MD 20084

Office of Naval Research
Code 473
800 N. Quincy Street
Arlington, VA 22217

Dr. L. A. Segel
Department of Mathematics
Rensselaer Polytechnic Institute
Troy, NY 12181

Professor J. L. Lumley
Department of Aerospace Engineering
Pennsylvania State University
University Park, PA 16802

Dr. J. M. Robertson
Department of Theoretical and Applied
Mechanics
University of Illinois
Urbana, IL 61803

Technical Library
Mare Island Naval Shipyard
Valleno, CA 94592

Office of Naval Research
Code 438
800 N. Quincy Street
Arlington, VA 22217 3 copies

Office of Naval Research
Code 200
800 N. Quincy Street
Arlington, VA 22217

Office of Naval Research
Code 210
800 N. Quincy Street
Arlington, VA 22217

Office of Naval Research
Code 211
800 N. Quincy Street
Arlington, VA 22217

Office of Naval Research
Code 212
800 N. Quincy Street
Arlington, VA 22217

Office of Naval Research
Code 221
800 N. Quincy Street
Arlington, VA 22217

Office of Naval Research
Code 480
800 N. Quincy Street
Arlington, VA 22217

Office of Naval Research
Code 481
800 N. Quincy Street
Arlington, VA 22217

Office of Naval Research
Code 1021P (ONRL)
800 N. Quincy Street
Arlington, VA 22217 6 copies

Naval Research Laboratory
Washington, D. C. 20375

Attn: Code 2627 - 6 copies
Code 4009
Code 7000 - 25 copies
Code 7750 - 75 copies
Code 8841 (R. J. Hansen)

Mr. L. Benen (Code 0322)
Naval Sea Systems Command
Washington, DC 20362

Mr. J. Schuler (Code 032)
Naval Sea Systems Command
Washington, DC 20362

Code 03B
Naval Sea Systems Command
Washington, DC 20362

Mr. T. Peirce (Code 03512)
Naval Sea Systems Command
Washington, DC 20362

Library (Code 09GS)
Naval Sea Systems Command
Washington, DC 20362

Professor C. E. Pearson
Aerospace Research Laboratory
University of Washington
Seattle, WA 98105

Dr. Steven Crow, President
Poseidon Research
11777 San Vicente Blvd., Suite 641
Los Angeles, CA 90049

Mr. J. Enig (Room 3-252)
Naval Surface Weapons Center
White Oak Laboratory
Silver Spring, MD 20910

Librarian
Naval Surface Weapons Center
White Oak Laboratory
Silver Spring, MD 20910

Mr. J. Rogers
Naval Surface Weapons Center
White Oak Laboratory
Silver Spring, MD 20910

Fenton Kennedy Document Library
The Johns Hopkins University
Applied Physics Laboratory
Johns Hopkins Rd.
Laurel, Md. 20180

Professor Milton van Dyke
Department of Aeronautical Engineering
Stanford University
Stanford, CA 94305

Professor J. Thompson
Department of Aerophysics and Aerospace
Engineering
Mississippi State University
State College, MS 39762

Professor R. DiPrima
Department of Mathematics
Rensselaer Polytechnic Institute
Troy, NY 12181

Army Research Office
P. O. Box 12211
Research Triangle Park, NC 27709

Dr. H. Norman Abramson
Southwest Research Institute
8500 Culebra Road
San Antonio, TX 78228

ONR Scientific Liaison Group
American Embassy - Room A-407
APO San Francisco 96503

Editor
Applied Mechanics Review
Southwest Research Institute
8500 Culebra Road
San Antonio, TX 78228

Dr. J. W. Hoyt
Code 2501
Naval Undersea Center
San Diego, CA 92132

Technical Library
Naval Undersea Center
San Diego, CA 92132

Dr. Andrew Fabula
Code 4007
Naval Undersea Center
San Diego, CA 92132

Office of Naval Research
San Francisco Area Office
760 Market Street, Room 447
San Francisco, CA 94102

Library
Peral Harbor Naval Shipyard
Box 400
FPO San Francisco 96610

Technical Library
Hunters Point Naval Shipyard
San Francisco, CA 94135

Professor A. Hertzberg
Director, Aerospace Research Laboratory
University of Washington
Seattle, WA 98105

Technical Library
Naval Missile Center
Point Mugu, CA 93041

Commander
Portsmouth Naval Shipyard
Portsmouth, NH 03801

Commander
Norfolk Naval Shipyard
Portsmouth, VA 23709

Mr. C. duP Donaldson Associates
Aeronautical Research of Princeton, Inc.
50 Washington Road
Princeton, N. J. 08540

Professor F. Hama
Department of Aerospace and
Mechanical Science
Princeton University
Princeton, NJ 08540

Dr. J. Clarke
Division of Engineering
Brown University
Providence, RI 02912

Professor J. Liu
Division of Engineering
Brown University
Providence, RI 02912

Dr. E. Baum
TRW Systems Group
One Space Park
Redondo Beach, CA 90278

Chief, Document Section
Redstone Scientific Information Center
Army Missile Command
Redstone Arsenal, AL 35809

Dr. A. Eshel
Ampex Corporation
401 Broadway
Redwood City, CA 94063

Professor M. S. Plesset
Engineering Science Department
California Institute of Technology
Pasadena, CA 91109

Professor A. Roshko
Graduate Aeronautical Laboratories
California Institute of Technology
Pasadena, CA 91109

Professor T. Y. Wu
Engineering Science Department
California Institute of Technology
Pasadena, CA 91109

Director
Office of Naval Research Branch Office
1030 E. Green Street
Pasadena, CA 91101

Mr. R. Wade
Tetra Tech., Inc.
Marine and Environmental Engineering Division
630 N. Rosemead Blvd.
Pasadena, CA 91107

Professor K. M. Agrawal
Virginia State College
Department of Mathematics
Petersburg, VA 23802

Technical Library
Naval Ship Engineering Center
Philadelphia Division
Philadelphia, PA 19112

Technical Library
Philadelphia Naval Shipyard
Philadelphia, PA 19112

Professor R. C. MacCamy
Department of Mathematics
Carnegie Institute of Technology
Pittsburgh, PA 15213

Dr. Paul Kaplan
Oceanics, Inc.
Technical Industrial Park
Plainview, NY 11803

Technical Library
Naval Underwater Systems Center
Newport, RI 02840

Office of Naval Research
New York Area Office
715 Broadway - Fifth Floor
New York, NY 10003

Professor J. J. Stoker
Courant Institute of Mathematical
Sciences
New York University
251 Mercer Street
New York, NY 10003

Professor V. Castelli
Department of Mechanical Engineering
Columbia University
New York, NY 10027

Professor H. G. Elrod
Department of Mechanical Engineering
Columbia University
New York, NY 10027

Engineering Societies Library
345 East 47th Street
New York, NY 10017

Society of Naval Architects and
Marine Engineers
74 Trinity Place
New York, NY 10006

Librarian, Aeronautical Laboratory
National Research Council
Montreal Road
Ottawa 7, Canada

Technical Library
Naval Coastal System Laboratory
Panama City, FL 32401

Professor H. W. Liepmann
Graduate Aeronautical Laboratories
California Institute of Technology
Pasadena, CA 91109

Director
Scripps Institute of Oceanography
University of California
La Jolla, CA 92037

Mr. Virgil Johnson, President
Hydronautics, Incorporated
7210 Pindell School Road
Laurel, MD 20810

Mr. M. P. Tulin
Hydronautics, Incorporated
7210 Pindell School Road
Laurel, MD 20810

Commander
Long Beach Naval Shipyard
Long Beach, CA 90801

Dr. C. W. Hirt
University of California
Los Alamos Scientific Laboratory
P. O. Box 1663
Los Alamos, NM 87544

Professor John Laufer
Department of Aerospace Engineering
University of Southern California
University Park
Los Angeles, CA 90007

Lorenz G. Straub Library
St. Anthony Falls Hydraulic Laboratory
University of Minnesota
Minneapolis, MN 55414

Dr. E. Silberman
St. Anthony Falls Hydraulic Laboratory
University of Minnesota
Minneapolis, MN 55414

Library
Naval Postgraduate School
Monterey, CA 93940

Professor J. Wu
College of Marine Studies
University of Delaware
Newark, DE 19711

Dr. J. P. Craven
University of Hawaii
1801 University Avenue
Honolulu, HI 96822

Professor F. Hussain
Department of Mechanical Engineering
Cullen College of Engineering
University of Houston
Houston, TX 77004

Professor J. F. Kennedy, Director
Institute of Hydraulic Research
University of Iowa
Iowa City, IA 52242

Professor L. Landweber
Institute of Hydraulic Research
University of Iowa
Iowa City, IA 52242

Professor E. L. Resler
Graduate School of Aerospace Engineering
Cornell University
Ithaca, NY 14851

Dr. D. R. S. Ko
Flow Research Inc.
1819 S. Central Avenue
Kent, WA 98031

Professor V. W. Goldschmidt
School of Mechanical Engineering
Purdue University
Lafayette, IN 47907

Professor J. W. Miles
Institute of Geophysics and Planetary
Physics, A-025
University of California, San Diego
La Jolla, CA 92093

Flow Research, Inc.
Los Angeles Division
9841 Airport Blvd., Suite 1004
Los Angeles, CA 90045

Dr. R. Chan
JAYCOR
1401 Camino Del Mar
Del Mar, CA 92014

Dr. J. A. Young
JAYCOR
1401 Camino Del Mar
Del Mar, CA 92014

Dr. R. H. Kraichnan
Dublin, NH 03444

Dr. Martin H. Bloom
Director of Gas Dynamics Research
Polytechnic Institute of New York
Long Island Center
Farmingdale, NY 11735

Research and Technology Division
Army Engineering Reactors Group
Fort Belvoir, VA 22060

Technical Documents Center
Building 315
Army Mobility Equipment Research Center
Fort Belvoir, VA 22060

Technical Library
Webb Institute of Naval Architecture
Glen Cove, NY 11542

Professor E. V. Lewis
Webb Institute of Naval Architecture
Glen Cove, NY 11542

Dr. M. Poreh
Technion-Israel Institute of Technology
Department of Civil Engineering
Haifa, Israel

Dr. J. P. Breslin
Davidson Laboratory
Stevens Institute of Technology
Castle Point Station
Hoboken, NJ 07030

Dr. S. Orszag
Flow Research, Inc.
1 Broadway
Cambridge, MA 02142

Dr. Edgar J. Gunter, Jr.
University of Virginia
School of Engineering and Applied
Science
Charlottesville, VA 22903

Director
Office of Naval Research Branch Office
536 South Clark Street
Chicago, ILL. 60605

Library
Naval Weapons Center
China Lake, CA 93555

Professor E. Reshotko
Division of Chemical Engineering Science
Case Western Reserve University
Cleveland, OH 44106

Commander
Charleston Naval Shipyard
Naval Base
Charleston, SC 29408

Professor J. M. Burgers
Institute of Fluid Dynamics and
Applied Mathematics
University of Maryland
College Park, MD 20742

Professor Pai
Institute for Fluid Dynamics and
Applied Mathematics
University of Maryland
College Park, MD 20740

Technical Library
Naval Weapons Surface Center
Dahlgren Laboratory
Dahlgren, VA 22418

Computation and Analyses Laboratory
Naval Weapons Surface Center
Dahlgren Laboratory
Dahlgren, VA 22418

Professor M. A. Abkowitz
Department of Ocean Engineering
Massachusetts Institute of Technology
Cambridge, MA 02139

Commanding Officer
NROTC Naval Administrative Unit
Massachusetts Institute of Technology
Cambridge, MA 02139

Professor L. N. Howard
Department of Mathematics
Massachusetts Institute of Technology
Cambridge, MA 02139

Professor Phillip Mandel
Department of Ocean Engineering
Massachusetts Institute of Technology
Cambridge, MA 02139

Professor C. C. Mei
Department of Civil Engineering
Massachusetts Institute of Technology
Cambridge, MA 02139

Professor E. Mollo-Christensen
Department of Meteorology
Room 54-1722
Massachusetts Institute of Technology
Cambridge, MA 02139

Professor J. Nicholas Newman
Department of Ocean Engineering
Room 5-324A
Massachusetts Institute of Technology
Cambridge, MA 02139

Professor R. F. Probstein
Department of Mechanical Engineering
Massachusetts Institute of Technology
Cambridge, MA 02139

Librarian
Department of Naval Architecture
University of California
Berkeley, CA 94720

Professor P. Lieber
Department of Mechanical Engineering
University of California
Berkeley, CA 94720

Professor P. Naghdi
College of Mechanical Engineering
University of California
Berkeley, CA 94720

Professor W. C. Webster
Department of Naval Architecture
University of California
Berkeley, CA 94720

Professor J. V. Wehausen
Department of Naval Architecture
University of California
Berkeley, CA 94720

Director
Office of Naval Research Branch Office
495 Summer Street
Boston, MA 02210

Commander
Puget Sound Naval Shipyard
Bremerton, WA 98314

Dr. Alfred Ritter
CALSPAN Corporation
P. O. Box 235
Buffalo, NY 14221

Professor G. Birkhoff
Department of Mathematics
Harvard University
Cambridge, MA 02138

Professor G. F. Carrier
Division of Engineering and
Applied Physics
Pierce Hall
Harvard University
Cambridge, MA 02138

Library
C. S. Draper Laboratory
68 Albany Street
Cambridge, MA 02139